Peer reviewed version of the manuscript published in final form in the Journal of the American Chemical Society, 2019, DOI: 10.1021/jacs.9b09899

A Dual Wavelength Polymerization and Bioconjugation Strategy for High Throughput Synthesis of Multivalent Ligands

Zihao Li,[1‡] Shashank Kosuri,[2‡] Henry Foster,[1] Jarrod Cohen,[3] Coline Jumeaux,[4,5] Molly M. Stevens,[4,5] Robert Chapman,*[1] Adam J. Gormley*[2]

[1]Centre for Advanced Macromolecular Design (CAMD) and the Australian Centre for Nanotechnology (ACN), School of Chemistry, UNSW, Sydney, Australia

[2]Department of Biomedical Engineering, Rutgers, The State University of New Jersey, Piscataway, NJ 08854, USA

[3]New Jersey Center for Biomaterials, Rutgers, The State University of New Jersey, Piscataway, NJ 08854, USA

[4]Department of Materials, Department of Bioengineering, and the Institute for Biomedical Engineering, Imperial College London, London SW7 2AZ, United Kingdom

[5]Division of Medical Biochemistry and Biophysics (MBB), Karolinska Institutet, Stockholm, Sweden

ABSTRACT: Structure-function relationships for multivalent polymer scaffolds are highly complex due to the wide diversity of architectures offered by such macromolecules. Evaluation of this landscape has traditionally been accomplished case-by-case due to the experimental difficulty associated with making these complex conjugates. Here, we introduce a simple dual-wavelength, two-step polymerize & click approach for making combinatorial conjugate libraries. It proceeds by incorporation of a polymerization friendly cyclopropenone-masked dibenzocyclooctyne (cp-DIBAC) into the side chain of linear polymers or the α-chain end of star polymers. Polymerizations are performed under visible light using an oxygen tolerant porphyrin-catalyzed photoinduced electron/energy transfer-reversible addition-fragmentation chain-transfer (PET-RAFT) process, after which the deprotection and click reaction is triggered by UV light. Using this approach, we are able to precisely control the valency and position of ligands on a polymer scaffold in a manner conducive to high throughput synthesis.

INTRODUCTION

Multivalent polymer and nanoparticle scaffolds are increasingly important in drug delivery, glycoscience, immunology, cancer therapy, and regenerative medicine because of their ability to interact with and control protein function.[1-14] The specificity and avidity of these large molecules comes not only from their size, but also their polyvalent display of ligands.[6, 8, 14-16] One challenge associated with the design of multivalent scaffolds is the very large diversity of available physicochemical characteristics. The size, valency, position of ligands, polymer chemistry, and architecture of the material will all dramatically affect function. Point substitution and chemical optimization of ligands on small-molecule scaffolds has been common practice for developing structure-activity relationships in medicinal chemistry for many years.[17-19] However, while modest efforts to explore the macromolecular landscape have been attempted, they are severely restricted in synthetic throughput.[3-5, 20]

Because of the incompatibility of many biologically relevant ligands, such as peptides, with controlled-radical polymerization (CRP) processes, complex polymer scaffolds are often functionalized after polymerization. To do this requires a conjugation strategy that is both efficient and compatible with high throughput polymer synthesis.[21-23] There are now several additive-free click reactions including Diels-Alder,[24] thiol-ene,[25, 26] tetrazine-based cycloadditions,[27-29] and strain promoted azide-alkyne cycloadditions (SPAAC) using cyclooctynes and dibenzocyclooctynes,[30-37] which avoid the use of potentially toxic catalysts such as copper. Many of these catalyst-free click reactions proceed very quickly in a wide range of solvents and do not produce reaction by-products. The overall stability of cyclooctynes and specificity for the azide reactive handle make SPAAC the most widely used catalyst-free click reaction in bioconjugations.[32] Cyclooctynes such as difluorocyclooctyne (DIFO),[31] as well as the more synthetically tractable dibenzylcyclooctynes (DBCO or DIBAC) and biarylazacyclooctynones (BARAC),[33-35] yield reaction rates of ~0.1 - 0.6 M^{-1} thanks to the electron withdrawing groups adjacent to the octyne. While these rates are lower than many tetrazine and Diels-Alder reactions, they are comparable with copper

Peer reviewed version of the manuscript published in final form in the Journal of the American Chemical Society, 2019, DOI: 10.1021/jacs.9b09899

catalyzed cycloadditions and sufficient to give quantitative click within hours at concentrations as low as 0.1-1 mM.

Unfortunately, these 'spring-loaded' chemical moieties tend not to be stable during free radical polymerization, resulting in both loss of click functionality and control over the polymerization. While CRPs can tolerate low concentration norbornene, its reactivity towards radicals will

Peer reviewed version of the manuscript published in final form in the Journal of the American Chemical Society, 2019, DOI: 10.1021/jacs.9b09899

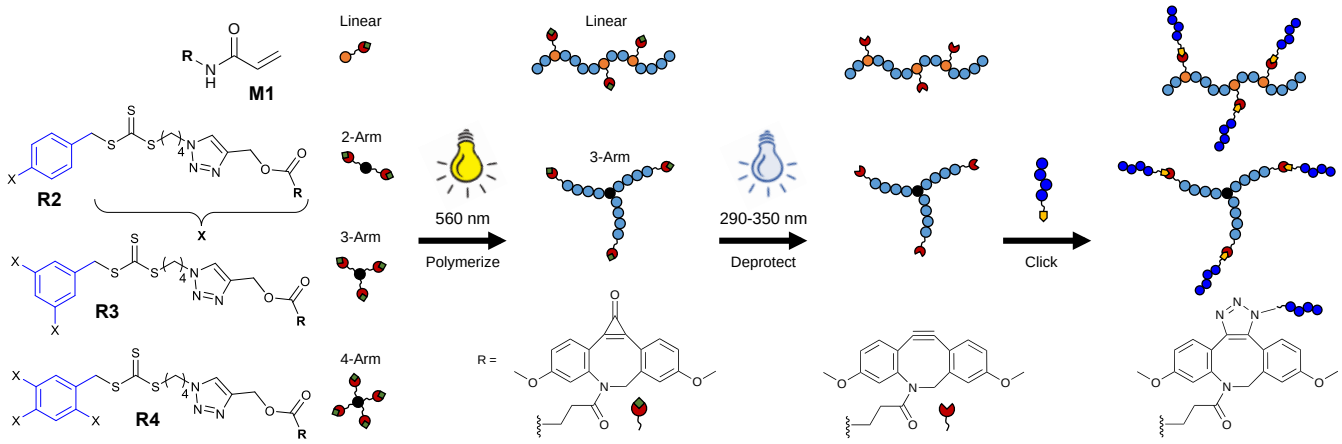

Figure 1. Reaction schematic. Cyclopropenone-masked DIBAC (cp-DIBAC) was synthesized either as a monomer (**M1**) or at the end of 2-arm (**R2**), 3-arm (**R3**), or 4-arm (**R4**) RAFT agents. Polymerization by PET-RAFT with 560 nm light followed by cp deprotection with UV produced SPAAC-ready polymer scaffolds for ligand clicking.

always result in some norbornene consumption during polymerization, particularly at high monomer conversion.[38, 39] For this reason most click functionalities need to be either chemically deprotected or introduced after polymerization, neither of which are compatible with high throughput approaches.[40, 41] Popik *et al.* recently developed a cyclopropenone-masked DIBAC (cp-DIBAC), which becomes photoactivated following UV deprotection of the cyclopropenone and generation of the strained alkyne.[42] The ability to unmask DIBAC with UV creates a photo-triggered click reaction that has since been used in several applications.[43-47] While originally introduced to simplify the synthesis of the molecule and to provide a photo-trigger, masking of DIBAC with the bulky cyclopropenone also renders the alkene compatible with free radical polymerizations. Zhang *et al.* leveraged this compatibility to incorporate a cp-DIBAC into the chain-end of linear polymers made by RAFT and atom transfer radical polymerization (ATRP) which they used to photo-trigger polymer cyclization.[48-51] Building on Zhang's encouraging findings, we sought to expand on cp-DIBAC's potential as a functional tool in polymer click chemistry.

Here, we present a simple one-pot, dual-wavelength procedure for preparing SPAAC-ready linear or star-shaped polymers for bioconjugation (**Figure 1**). This study builds on our previous work in the development of oxygen-tolerant CRP techniques for combinatorial polymer library production.[52-57] In this work we use the PET-RAFT polymerization method developed by Boyer and coworkers to form libraries in well-plates using 560 nm photoexcitation.[57-62] We incorporate cp-DIBAC either into the side chain of linear polymers by statistical copolymerization, or into the Z group of star RAFT agents prior to polymerization, thus enabling the synthesis of end-functional star polymers. Because star polymers present exactly the same number of ligands from each scaffold the biological effect of 2, 3 and 4 ligands can be compared, alongside the effect of polymer size. Subsequent deprotection of the cp group at an orthogonal wavelength (350 nm) followed by click addition of azido ligands results in the preparation of biofunctional polymers. The combination of these simplified procedures creates an overall versatile and robust tool for making biofunctional polymers for the non-expert.

EXPERIMENTAL

Materials and synthetic procedures: Detailed synthetic methods and characterization of the cp-DIBAC, cp-DIBAC monomer (**Figures S1-S5**) and the star RAFT agents are given in the supporting information. The peptide GEVC (GEVCLTSCSRLR-PEG$_2$-K(N$_3$)-CONH$_2$),[63] was purchased from China Peptides with >95% purity as measured by LCMS. The remaining two peptides BMP (K(N$_3$)-PEG$_2$-KIPKASSVPTELSAISTLYL-CONH$_2$),[64] and QK (KLTWQELYQLKYKGI-PEG$_2$-K(N$_3$)-CONH$_2$),[65] were synthesized on the solid phase (rink-amid resin) using a CEM Liberty Blue automated microwave peptide synthesizer (CEM Corporation). Following deprotection and cleavage from the resin, peptides were purified using a C18 column and a gradient of acetonitrile. Purity and mass were confirmed by HPLC and MS.

General procedure to prepare linear polymers with cp-DIBAC monomer (M1): Stock solutions of monomer (2 M), cp-DIBAC (45 mM), 4-cyano-4-[(dodecylsulfanylthiocarbonyl) sulfanyl]pentanoic acid (RAFT agent, 0.05 M) and ZnTPP (2 mM) were prepared in DMSO and pipetted into 384-well clear flat-bottom white plates (Greiner bio-one) while keeping the ZnTPP/CTA ratio at 0.01, varying monomer/CTA ratio and monomer/cp-DIBAC ratio depending on the target degree of polymerization (DP), as well as the amount of cp-DIBAC incorporation desired in the final polymer composition. The mixtures were then diluted with DMSO to a final volume of 100 µL and final monomer concentration at 0.5 M. Mixtures were covered with well-plate sealing tape to prevent evaporation and irradiated under 560 nm LED light for 18 h (5 mW/cm^2, TCP 12 Watt Yellow LED BR30 bulb). Despite non-uniform lighting of each well from the bulb, we find that full conversion is obtained for each polymer after an overnight reaction.

Polymer purification: Linear polymers were purified using Sephadex G-25 spin columns to remove any unreacted cp-DIBAC before deprotection and click addition. Briefly, Sephadex G-25 super fine powder (Sigma Aldrich) was dissolved in DMSO (37.5 mg/mL) and allowed to sit for at least 3 h at room temperature for the resin to swell. 0.5 mL Zeba spin columns (Thermo Fisher) were loaded manually with the resin and washed three times with DMSO at 1000 *g* for 1 min. After washing, 60 µL of polymer crude was added

Peer reviewed version of the manuscript published in final form in the Journal of the American Chemical Society, 2019, DOI: 10.1021/jacs.9b09899

on top of the resin and centrifuged at 1000 *g* for 2 min to obtain the purified sample. UV-Vis spectral absorbance (250-400 nm) of polymer sample before and after purification (2 μL in

Peer reviewed version of the manuscript published in final form in the Journal of the American Chemical Society, 2019, DOI: 10.1021/jacs.9b09899

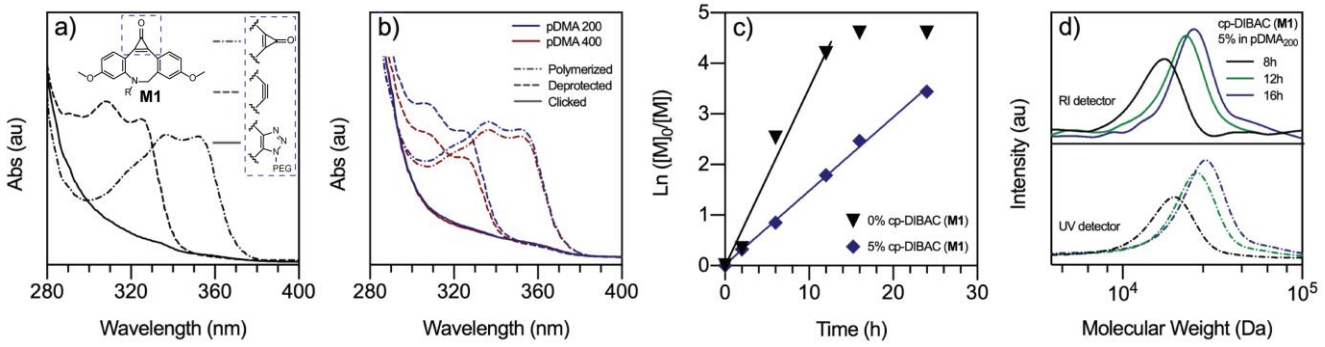

Figure 2. UV-Vis of cp-DIBAC and polymerization kinetics. a) UV-Vis of cp-DIBAC monomer (**M1**) before and after deprotection showing blue-shift of the characteristic peak, followed by a loss in absorbance after click to 2kDa PEG-N_3. b) UV-Vis traces of pDMA with 5% (mol) cp-DIBAC monomer (**M1**) incorporated at DP 200 and 400 before and after deprotection, and following click to 2kDa PEG-N_3. c) Kinetics of PET-RAFT polymerization with and without cp-DIBAC monomer (**M1**) showing complete conversion in both cases after 16h**.** d) GPC traces for pDMA with 5% (mol) cp-DIBAC monomer (**M1**) after 8, 12 and 16h of polymerization, showing incorporation of the cp-DIBAC by UV detection at 265 nm.

98 µL DMSO for measurement) were collected to calculate the percentage of cp-DIBAC removed.

Deprotection: Purified polymer was further diluted in DMSO to a final cp-DIBAC concentration of 5 mM into a 96-well polystyrene flat bottom plate (Denville) with a total volume of 40 µL. Deprotection of cp-DIBAC was completed by placing the 96-well plate under a 365 nm Spectroline (R) E-series UV-lamp (Sigma Aldrich) for 15 min. Deprotection was confirmed by UV-Vis spectroscopy.

Clicking: Conjugation of 2kDa PEG-N_3 onto polymers was achieved following a similar procedure to the deprotection, but in the presence of one equivalence of PEG-N_3 (50 mM in DMSO) with respect to cp-DIBAC. Solutions were left overnight at room temperature to allow complete conjugation. A UV-Vis spectrum was collected at the end of reaction time to confirm PEG addition.

General procedures to prepare star polymers: Stock solutions of star RAFT agents (0.1 M for CTA), monomer (2 M) and ZnTPP (4 mM) were prepared in DMSO and pipetted into 384 well clear flat-bottom black plates (Corning) to keep ZnTPP/CTA ratio at 0.01 and varying monomer/star RAFT agent ratio with desired targeting DP. The mixtures were then diluted with DMSO to make the total volume 40 µL and final DMA concentration 0.5 M. For 4-armed polymers, *N*-methyl-2-pyrrolidone (NMP, 8 µL) was added to the mixture before dilution with DMSO in order to suppress star-star coupling during polymerization. Mixtures were covered with well-plate sealing tape to prevent evaporation and irradiated under 560 nm LED light (Thorlabs M565L3, 2 mW/cm^2, **Figure S28**) for 18 h. A collimated lens was used to ensure even light irradiation across all samples. The resulting polymer solutions were processed directly for deprotection and click reactions without purification.

Deprotection: Aliquots of polymer solutions were transferred into PCR tubes and diluted with DMF to get cp-DIBAC concentration at 3 mM with total volume of 20 µL. Deprotection of cp-DIBAC was completed by exposing the PCR tubes to 290-350 nm UV light (Cosmedico ARIMED B6, 0.372 mW/cm^2, **Figure S28**) for 15 min.

Click: Conjugation of 2kDa PEG-N_3 onto polymers was achieved following a similar procedure to the deprotection, but in the presence of one equivalence of PEG-N_3 (100 mM in DMSO) with respect to cp-DIBAC. After UV deprotection, click samples were left in ambient environment overnight to allow complete conjugation.

RESULTS AND DISCUSSION

We began by exploring the synthesis of a cp-DIBAC functionalized monomer (**M1**), which was incorporated into linear polymers by a statistical copolymerization. This monomer was prepared following a procedure modified from literature (**Scheme S1**),[37] by addition of acryloyl chloride to the dibenzyl precursor (**2**) followed by cyclization of the dibenzocyclooctyne (**3**) with tetrachlorocyclopropene. The linker between cp-DIBAC and the acrylamide group was necessary to enhance DMSO solubility and provide space from the polymer chain. Most of the steps proceeded with good yield except the last cyclization step which generally provided 30% yield which is consistent with previously reported values,[42] except in cases of ultraconservative purification of **M1** (11%). In general, we found that monomer purity was critical as the presence of trace contaminants led to reduced polymerization kinetics. Despite this low yield, we do not find that this limits throughput and scalability due to the low volume of each reaction. Detailed synthesis information can be found in the supporting information.

The spectra of cp-DIBAC, deprotected DIBAC and DIBAC-azide allow for monitoring of these steps by UV-Vis. cp-DIBAC has a characteristic, two-hump peak between 340-360 nm which quickly drops off above 370 nm (**Figure 2a**). Deprotection of the cyclopropenone group with UV (290-350 nm) results in a 30 nm blue shift of this spectra with a new peak between 310-330 nm. Complete conversion to the deprotected DIBAC can be followed by monitoring for remaining absorbance above 350 nm. Subsequent addition of azide results in a fast click reaction and near complete loss of these peaks (**Figure 2a**). This convenient method therefore allows for online monitoring of the click reaction and for calculating the final concentration of cp-DIBAC against calibrated concentration standards.

Linear Polymers

Linear polymers with cp-DIBAC in the side chains were prepared in 384 or 96 well plates by PET-RAFT

copolymerization using ZnTPP as the photoinitiator in DMSO.[57] Monomer concentration was varied between 1.0 and 0.5 M, and ZnTPP/CTA ratio was fixed at 0.01 or 0.02 depending on the desired kinetics and conversion. The stock concentration of cp-DIBAC monomer (**M1**) was 45 mM as this is the solubility limit in DMSO. PET-RAFT polymerization was conducted under a yellow lamp overnight to achieve full conversion. If desired, relative polymerization conversion can be followed by the ratio of the ZnTPP fluorescence emission intensities at 632 and 615 nm.[66] After polymerization, the polymers were purified to remove any free cp-DIBAC and deprotected under UV for 15-25 minutes. During this time, deprotection was followed every five minutes by UV-Vis to verify complete deprotection. After deprotection, the concentration of DIBAC was calculated by UV-Vis and 1:1 equivalents of azide / DIBAC was added. Click was verified by UV-Vis and was typically complete within one hour.

The PET-RAFT copolymerization had no effect on cp-DIBAC and its subsequent deprotection and click as verified by UV-Vis (**Figure 2b**) and NMR (data not shown). Copolymerization showed adequate evolution of molecular weight with slightly delayed kinetics (**Figure 2c**). We hypothesize that this slight delay may be due to residual and difficult to remove impurities, but this has not been confirmed. Nonetheless, if left overnight, copolymerization with cp-DIBAC proceeds to >90% conversion. For example, when *N,N*-dimethyacrylamide (DMA) was copolymerized (DP 200 or 400) with 5 mol% cp-DIBAC, molecular weights were 29,091 ($Đ$ = 1.15) and 55,032 ($Đ$ = 1.27) Daltons, respectively (**Figure 3a, Table S1**). After clicking with 2kDa PEG-N_3, these molecular weights shifted to 41,758 ($Đ$ = 1.29) and 82,041 ($Đ$ = 1.34) Daltons. This indicates that approximately 7 and 14 PEGs were clicked to the DP 200 and DP 400 polymers, respectively. These click additions match the theoretical number of PEGs that would be clicked at 70% functionalization indicating remarkable control of post-polymerization modification. We also found that cp-DIBAC was tolerant to a number of monomers including 2-hydroxyethyl acrylate (HEA) (**Figure 3b**), 4-acryloyl morpholine (NAM) and *N*-isopropylacrylamide (NIPAM) (**Figure S22**). Evaluation of 2.5, 5, and 7.5% cp-DIBAC copolymerization also shows a reasonable range of obtainable valency with increasing comonomer input (**Figure 3c**). We were not able to go higher than 7.5% due to solubility limitations in DMSO, however, sulfonation of the cp-DIBAC could be used to facilitate greater solubility if desired.[44] Because of the strong UV extinction coefficient of cp-DIBAC, the UV trace from the GPC provided a reliable indicator of incorporation into the polymer chain (**Figure 3d**). We assume that the earlier GPC elution time for polymers with greater valency was due to collapse of the polymer chain in GPC eluent (DMF) due to the increased cp-DIBAC content. By NMR, all polymers (0, 2.5, 5, and 7.5%) proceeded to full conversion with narrow dispersity and should therefore have similar molecular weights.

Taking advantage of the cp protected DIBAC, we decided to see if this strategy could allow for dual ligand functionalization using the same SPAAC chemistry. This follows previous work by the authors in which we first copolymerized NHS-acrylate into a polymer by PET-RAFT, and then chemically conjugated DBCO-NH_2 to provide a polymer-DBCO conjugate.[57] Note that in this case, polymer-DBCO is SPAAC ready. To extend this in the present work we copolymerized 95% (mol) of a non-active monomer (DMA) with 2.5% NHS-acrylate and 2.5% cp-DIBAC to make a random heteropolymer with two different DIBACs (one protected and one unprotected). The first addition of PEG-N_3 by clicking to DBCO provided a predictable shift in molecular weight (**Figure 4a**) as well as a drop in the UV signal for DBCO at 318 nm (**Figure 4b**). Deprotection of cp-DIBAC with UV followed by the second PEG-N_3 addition resulted in another molecular weight shift and reduction in UV absorption from DIBAC. This indicates that we were able to dual functionalize polymers using SPAAC in both cases. This capability is very interesting as it allows for polymers to be functionalized with multiple ligands using by SPAAC. For example, when designing mucin mimetics, it is often desirable to label multivalent polymers with several different glycans in order to mimic the complex chemistry of most glycoproteins.[67]

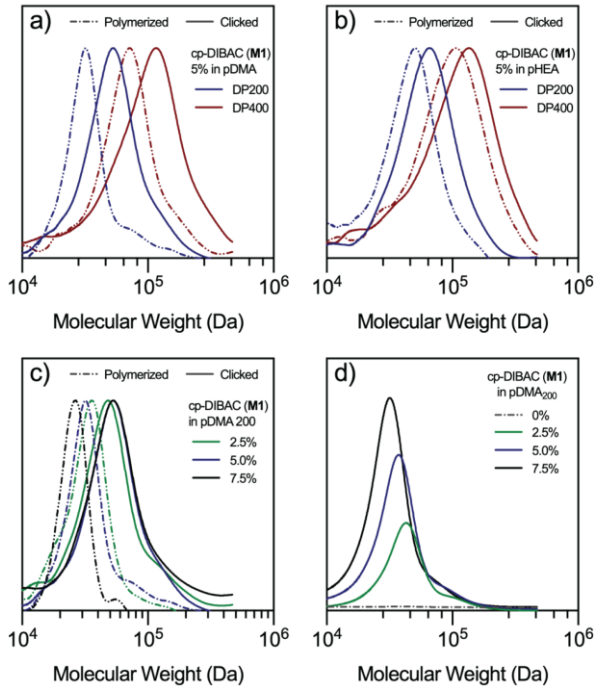

Figure 3. GPC traces showing the copolymerization of cp-DIBAC monomer (1) into side-chain functionalized linear polymers followed by click with 2kDa PEG-N_3. a) DMA with 5% cp-DIBAC, b) HEA with 5% cp-DIBAC, and c) DMA DP 200 with 2.5 – 7.5% cp-DIBAC. d) UV signal at 265 nm from GPC showing increasing incorporation of cp-DIBAC as a function of feed ratio.

Peer reviewed version of the manuscript published in final form in the Journal of the American Chemical Society, 2019, DOI: 10.1021/jacs.9b09899

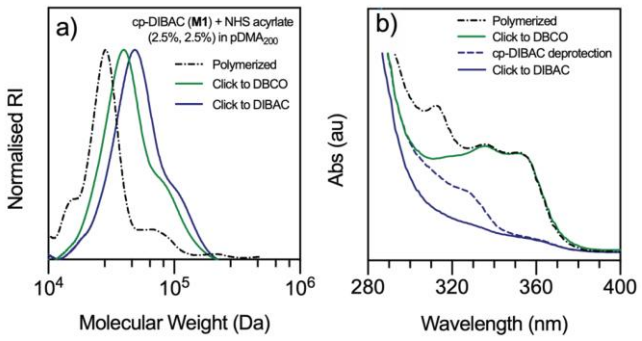

Figure 4. Dual functionalization by SPAAC. a) GPC traces after copolymerization of DMA / NHS-acrylate / cp-DIBAC (95 / 2.5 / 2.5 mol%) and addition of DBCO-NH_2 to create dual SPAAC-ready polymers. Subsequent click to DBCO, deprotection and secondary click of 2kDa PEG-N_3 to cp-DIBAC are shown in the green and blue lines respectively. b) UV-Vis traces of the protected polymer before and after the first DBCO click, after deprotection of the cp-DIBAC and after subsequent click to the DIBAC.

Star Polymers

Having demonstrated the chemistry in linear polymers we moved on to using cp-DIBAC to prepare end-functional star polymers. By placing cp-DIBAC at the ends of the star architecture, exact control over the number of ligands presented per polymer is achieved. The synthetic scheme for accessing star RAFT agents end functionalized with cp-DIBAC at the R group is depicted in **Scheme S4**. An alkyne group was first installed on cp-DIBAC via a similar synthetic route to that of the monomer **M1** (**Scheme S2**). Succinic anhydride was first ring-opened with propargyl alcohol and then coupled to the dibenzyl precursor (**1**) by amidation. Cyclization of the dibenzocyclooctyne with tetrachlorocyclopropene resulted in the alkyne functionalized cp-DIBAC (**7**) which could be attached to the star RAFT agents. The precursor azido-ended star RAFT agents (**10**, **12** and **14**) were synthesized by substitution of bromo groups with thiols in the corresponding bromomethyl benzene molecules[68] followed by sequential addition of carbon disulfide and 1-azido-4-bromobutane. Bromotris(triphenylphosphine) copper (I) catalyzed click reactions between the star RAFT agent's alkyne and cp-DIBAC (**7**) produced the desired star RAFT agents (**R2**, **R3** and **R4**). Detailed information about the synthesis optimization can be found in the supporting information.

The quantitative deprotection and click of the RAFT agents was observed by ^{1}H-NMR spectroscopy, as shown in **Figure 5** for the 3-arm example (**R3**), and in the supporting information (**Figures S19 and S20**) for the 2- and 4-arm examples (**R2** and **R4**). Upon irradiation (290-350 nm, 3 h) at 15 mM in *d6*-DMSO, the phenol peaks within the cp-DIBAC group shifted downfield by >0.5 ppm. Interestingly the triazole protons, despite their distance from the cp-DIBAC groups, shifted from 8.02 ppm to 8.06 ppm (**Figure 5a and 5b**). The results suggested a significant change in chemical environment due to the deprotection of cp-DIBAC from the cyclopropenone mask. After deprotection, quantitative click was observed after addition of 1 equivalence of O-(2-azidoethyl) heptaethylene glycol (400 PEG-N_3) relative to DIBAC, as evidenced again by ^{1}H NMR. The signal from the triazole protons at 8.06 ppm split into two peaks at 7.99 and 8.09 ppm with approximately the equal integration (**Figure 5c**) due to the mixture of regioisomers, consistent with previous reports.[30, 45] It is important to note that the trithiolcarbonate groups responsible for polymerizations were undamaged during these processes, as evidenced by the unaffected peak of the adjacent protons at 4.59 ppm (**Figure 5**). The same experiments were conducted with 2- and 4-arm star RAFT agents (**R2** and **R4**) and displayed consistent results (**Figures S19 and S20**).

ZnTPP initiated PET-RAFT polymerizations of star RAFT agents were prepared in a 384 well plate with total volume of 40 μL for each reaction mixture. The ZnTPP/CTA ratio was kept at 0.01, and 0.5 M DMA was used as the monomer. By controlling the ratio of monomer to star RAFT agents, two sets of polymerizations with targeting total DPs of 200 and 400 were prepared for each star RAFT agents. 2- and 3-arm RAFT agents were polymerized in DMSO, but the same conditions for the 4-arm RAFT agent resulted in a large degree of star-star coupling. We believe this is due to coordination of the ZnTPP by the polymer, as introduction

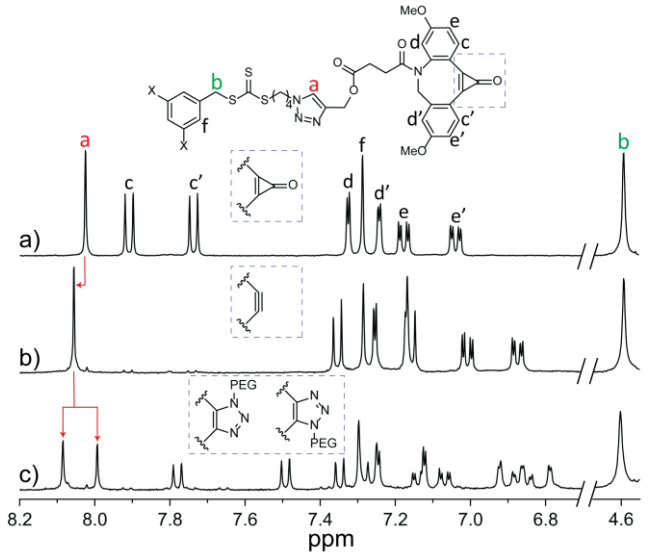

Figure 5. Deprotection and click of 3-arm star RAFT agent (3) by ^{1}H NMR (*d6*-DMSO). a) Before and b) after deprotection (3h UV) and c) after addition of 1.0 eq of 400 g.mol^{-1} PEG-N_3 with respect to DIBAC.

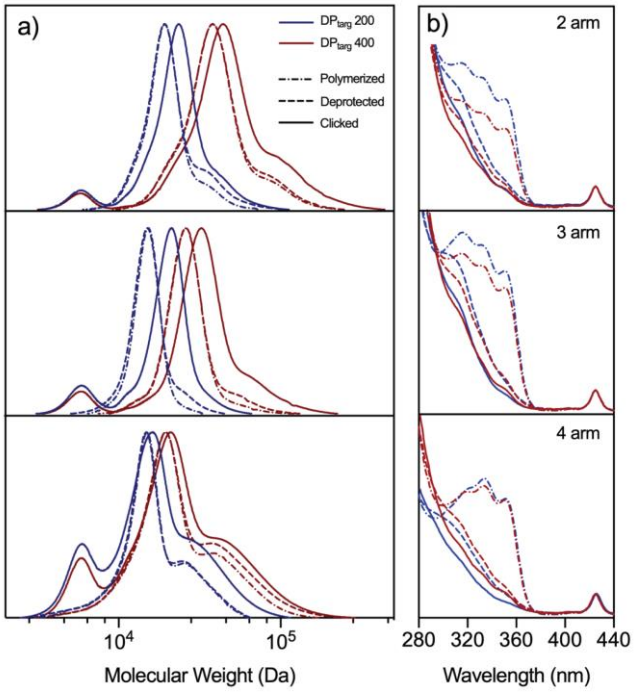

Figure 6. Polymerization, deprotection and SPAAC on star polymers. a) GPC and b) UV-Vis traces of DP_{targ} 200 and 400 pDMA using 2 (top), 3 (middle) and 4 (bottom) armed RAFT agents before and after deprotection and after addition of 1.0 eq of 2kDa PEG-N_3 with respect to DIBAC.

of 20% (v/v) *N*-methyl-2-pyrrolidone (NMP) suppressed this phenomenon (**Figure 6a**) resulting in star polymers of nearly monomodal molecular weight distributions. In a 384 well plate, the reaction mixtures were photoinitiated and allowed to polymerize for 18 hours. After polymerization, fractions of each sample were taken and diluted into two solutions with the final cp-DIBAC concentrations as 2.5 mM. The first solution was added with 1 equivalent 2kDa PEG-N_3 relative to cp-DIBAC prior to dilution and labeled as "click". The second solution contains the same mixture but without 2kDa PEG-N_3 and labeled as "deprotection". Deprotection of cp-DIBAC was carried out by radiating all solutions under UV light (290-350 nm) for 15 min while the click solutions were kept in ambient environment overnight to allow complete conjugation before measurements. GPC and UV-Vis measurements for polymerized, deprotected and clicked samples were conducted and compared accordingly (**Figure 6 and Table S2**).

PET-RAFT polymerizations with the star RAFT agents in well plates produced well controlled star polymers with narrow dispersities ($Đ$ < 1.35), particularly for the 3-arm polymers, having dispersities of 1.04 and 1.10 for target DPs of 200 and 400 respectively (**Table S2**). With the dilution of cp-DIBAC concentrations to 2.5 mM, the time required for complete deprotection was significantly reduced to 15 minutes as shown by UV-Vis (**Figure 6b**), compared to 3 hours for 15 mM cp-DIBAC from the NMR studies. More importantly, UV deprotection of cp-DIBAC does not re-initiate polymerization with the excess monomers presented in the mixtures, since there is no observable shift of GPC traces and only minor star-star coupling as indicated by small increases in higher molecular weight shoulders (**Figure 6a**). After deprotection and overnight incubation in ambient environment, the click samples displayed quantitative conjugation for polymers as loss of DIBAC peaks on UV-Vis (**Figure 6b**) and complete shift of GPC traces to higher molecular weight (**Figure 6a**). The new peaks displayed in the lower molecular weight regions are due to small amounts of excess unreacted PEG-N_3 in the mixture. This is because it is difficult to control 1:1 stoichiometry of 2 kDa PEG-N_3, which is a polymer, to DIBAC. DMSO solutions of star polymer-ligand conjugates can be purified easily by spin filtration with Sephadex where necessary.

Click Versatility and High Throughput

To show the versatility of this technique for preparing functional polymer conjugates we explored the efficiency of the click reaction with a range of more complicated peptides. We chose to test three different bioactive peptides (12-20 amino acids) which were modified to contain an azide at either the C or N terminus: a TRAIL mimicking peptide 'GEVC' (GEVCLTSCSRLR-PEG_2-K(N_3)-$CONH_2$),[63] a bone morphogenic protein mimicking peptide 'BMP' (K(N_3)-PEG_2-KIPKASSVPTELSAISTLYL-$CONH_2$),[64] and a VEGF mimicking peptide 'QK' (KLTWQELYQLKYKGI-PEG_2-K(N_3)-$CONH_2$).[65] A 2-arm pDMA (DP20) polymer was prepared following the general procedures for star polymers from the 2-arm RAFT agent (**R2**), using 200 µL *d6*-DMSO as the solvent and 10 h reaction time. This resulted in a conversion of 86% and a dispersity of 1.05. After mixing with 1.0 equiv peptide / cp-DIBAC and UV deprotection, quantitative conjugation of all four substrates was observed by a complete shift of the polymer peak in the LC-MS with a concurrent loss of signal from the substrate (**Figure 7a**). The identification of the polymer peaks was confirmed from their mass spectra (**Figure S23**). In the PDA spectra, the polymer peak can be seen to lose its characteristic absorbance at 350 nm (which comes from the protected cp-

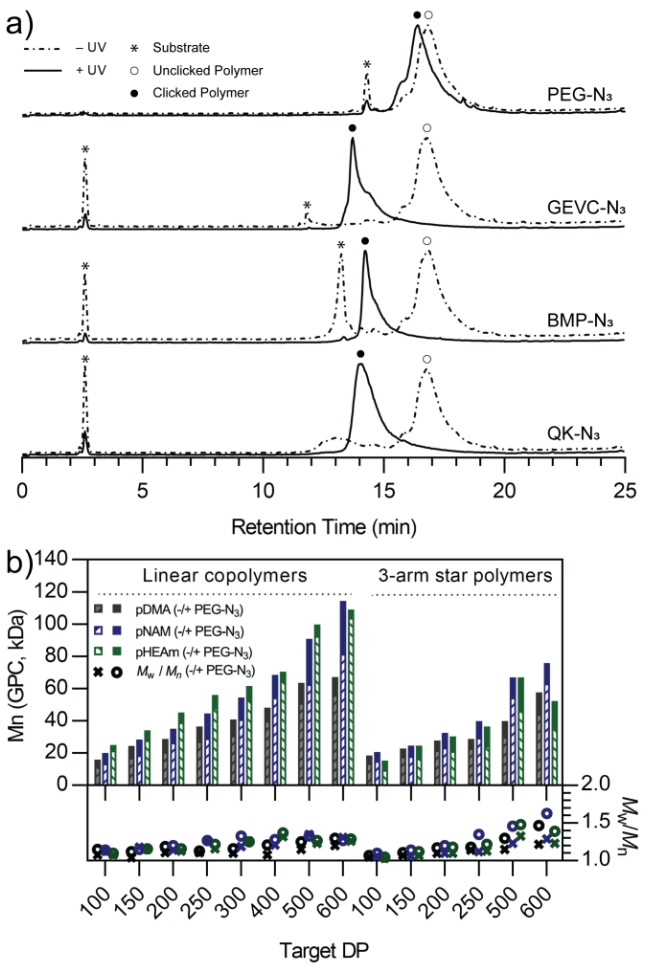

Figure 7. Scope of click and high throughput reactions a) Total positive ion count (TIC+) LC-MS data for mixtures of a 2-arm DP20 pDMA with 400 Da PEG-N_3 and three different peptides, with and without irradiation with UV light. Peaks corresponding to the polymer before (○) and after (●) click as well as the substrate peaks (*) are highlighted. b) Summary of GPC M_n and $Đ$ data high throughput polymer library of pDMA, pNAM and pHEAm linear copolymers (5% cp-DIBAC) and 3-arm star polymers before and after click with 2 kDa PEG-N_3. Full LC-MS data and GPC traces for each polymer are shown in the supporting information.

DIBAC) after deprotection and click (**Figure S24**). ^{1}H-NMR (**Figure S25**) confirms these results for each substrate, by the disappearance of the cp-DIBAC peaks associated with both the protected and deprotected polymers, and appearance of peaks corresponding to the clicked products.

Finally, we applied this system to synthesize a library of over 80 polymers and polymer conjugates to validate its high throughput capability (**Figure 7b**). Polymerization and click of linear and multi-arm polymers were performed in single wells of 384 well plates. The resulting polymers and their conjugates demonstrated excellent control of molecular weight, dispersity, conversion and click (**Figures S26-S27 and Table S6**). Overall, the methodology to produce this large library was not manually intensive and required small amounts of starting material (**M1**, **R2-4**) due to the small scale of this reaction. Further scaling of library size would therefore be straightforward to implement if desired.

CONCLUSIONS

We have presented a simplified, dual wavelength, one pot strategy for making multivalent polymers. It takes advantage of the tolerance of cp-DIBAC to radical polymerizations as well as well plate format PET-RAFT to make a highly versatile synthetic platform. We have shown this to work with linear polymers whose ligands are in the side chains as well as star polymers that are end-functionalized. Additional use of DBCO provides a simple avenue for functionalizing multiple ligands to single polymers using the same SPAAC click chemistry for each ligand. Therefore, using this synthetic technique, one can imagine making very large and diverse libraries of multivalent polymers with relative ease. Moving forward, we anticipate that this will enable non-experts to attempt this simple chemistry once cp-DIBAC becomes accessible to non-chemists.

ASSOCIATED CONTENT

Supporting Information

Detailed methods, cp-DIBAC characterization and additional results can be found in Supporting Information. The Supporting Information is available free of charge on the ACS Publications website.
Supporting_Information.pdf

AUTHOR INFORMATION

Corresponding Author

* Adam J. Gormley: Adam.Gormley@rutgers.edu
* Robert Chapman: r.chapman@unsw.edu.au

Present Addresses

Author Contributions

‡These authors contributed equally to the work.

Funding Sources

This work was supported by a Rutgers Global Collaborative Research Grant and a Busch Biomedical Award to AJG. RC is grateful to the Australian Research Council for funding through a Discovery Early Career Researcher Award (DECRA, DE170100315).

Notes

Any additional relevant notes should be placed here.

ACKNOWLEDGMENT

A.J.G. would like to thank Inês Albino, Laura Tiemeijer and Chris Spicer for their contributions to cp-DIBAC synthesis and characterization. Jarrod Cohen is a graduate student in the laboratory of Professor Joachim Kohn at Rutgers University and was supported by the New Jersey Center for Biomaterials.

ABBREVIATIONS

CRP, controlled radical polymerization; cp-DIBAC, cyclopropenone-masked dibenzocyclooctyne; PET-RAFT, porphyrin-

catalyzed photoinduced electron/energy transfer-reversible addition-fragmentation chain-transfer; SPAAC, strain promoted azide-alkyne cycloaddition.

REFERENCES

1. Seferos, D. S.; Prigodich, A. E.; Giljohann, D. A.; Patel, P. C.; Mirkin, C. A. Polyvalent DNA Nanoparticle Conjugates Stabilize Nucleic Acids. *Nano Letters* **2009,** 9 (1), 308-311 DOI: 10.1021/nl802958f.
2. Giljohann, D. A.; Seferos, D. S.; Patel, P. C.; Millstone, J. E.; Rosi, N. L.; Mirkin, C. A. Oligonucleotide Loading Determines Cellular Uptake of DNA-Modified Gold Nanoparticles. *Nano Letters* **2007,** 7 (12), 3818-3821 DOI: 10.1021/nl072471q.
3. Lynn, G. M.; Laga, R.; Darrah, P. A.; Ishizuka, A. S.; Balaci, A. J.; Dulcey, A. E.; Pechar, M.; Pola, R.; Gerner, M. Y.; Yamamoto, A. In vivo characterization of the physicochemical properties of polymer-linked TLR agonists that enhance vaccine immunogenicity. *Nature biotechnology* **2015,** 33 (11), 1201 DOI: https://doi.org/10.1038/nbt.3371.
4. Cairo, C. W.; Gestwicki, J. E.; Kanai, M.; Kiessling, L. L. Control of multivalent interactions by binding epitope density. *Journal of the American Chemical Society* **2002,** 124 (8), 1615-1619 DOI: https://doi.org/10.1021/ja016727k.
5. Gestwicki, J. E.; Cairo, C. W.; Strong, L. E.; Oetjen, K. A.; Kiessling, L. L. Influencing receptor-ligand binding mechanisms with multivalent ligand architecture. *Journal of the American Chemical Society* **2002,** 124 (50), 14922-14933 DOI: https://doi.org/10.1021/ja027184x.
6. Mammen, M.; Choi, S.-K.; Whitesides, G. M. Polyvalent Interactions in Biological Systems: Implications for Design and Use of Multivalent Ligands and Inhibitors. *Angewandte Chemie International Edition* **1998,** 37 (20), 2754-2794 DOI: https://doi.org/10.1002/(SICI)1521-3773(19981102)37:20%3C2754::AID-ANIE2754%3E3.0.CO;2-3.
7. Kwon, S.-J.; Na, D. H.; Kwak, J. H.; Douaisi, M.; Zhang, F.; Park, E. J.; Park, J.-H.; Youn, H.; Song, C.-S.; Kane, R. S.; Dordick, J. S.; Lee, K. B.; Linhardt, R. J. Nanostructured glycan architecture is important in the inhibition of influenza A virus infection. *Nat Nano* **2017,** 12 (1), 48-54 DOI: 10.1038/nnano.2016.181.
8. Krishnamurthy, V. M.; Estroff, L. A.; Whitesides, G. M., Multivalency in Ligand Design. In *Fragment-based Approaches in Drug Discovery*, Mannhold, R., Kubinyi, H., Folkers, G., Jahnke, W., Erlanson, D. A., Eds. 2006; pp 11-53.
9. Harrison, R. H.; Steele, J. A. M.; Chapman, R.; **Gormley, A. J.**; Chow, L. W.; Mahat, M. M.; Podhorska, L.; Palgrave, R. G.; Payne, D. J.; Hettiaratchy, S. P.; Dunlop, I. E.; Stevens, M. M. Modular and Versatile Spatial Functionalization of Tissue Engineering Scaffolds through Fiber-Initiated Controlled Radical Polymerization. *Advanced Functional Materials* **2015,** 25 (36), 5748-5757.
10. Conway, A.; Vazin, T.; Spelke, D. P.; Rode, N. A.; Healy, K. E.; Kane, R. S.; Schaffer, D. V. Multivalent ligands control stem cell behaviour in vitro and in vivo. *Nature Nanotechnology* **2013,** 8 (11), 831-838.
11. Chu, T.-W.; Kopecek, J. Drug-free macromolecular therapeutics - a new paradigm in polymeric nanomedicines. *Biomaterials Science* **2015,** 3 (7), 908-922 DOI: 10.1039/C4BM00442F.
12. Bennett, N. R.; Zwick, D. B.; Courtney, A. H.; Kiessling, L. L. Multivalent antigens for promoting B and T cell activation. *ACS Chemical Biology* **2015,** 10 (8), 1817-1824.
13. Clayton, R.; Hardman, J.; LaBranche, C. C.; McReynolds, K. D. Evaluation of the Synthesis of Sialic Acid-PAMAM Glycodendrimers without the Use of Sugar Protecting Groups, and the Anti-HIV-1 Properties of These Compounds. *Bioconjugate Chemistry* **2011,** 22 (10), 2186-2197 DOI: 10.1021/bc200331v.
14. Tjandra, K. C.; Thordarson, P. Multivalency in Drug Delivery–When Is It Too Much of a Good Thing? *Bioconjugate Chemistry* **2019,** 30, 503-514 DOI: 10.1021/acs.bioconjchem.8b00804.
15. Ercolani, G.; Schiaffino, L. Allosteric, Chelate, and Interannular Cooperativity: A Mise au Point. *Angewandte Chemie International Edition* **2011,** 50 (8), 1762-1768 DOI: 10.1002/anie.201004201.
16. Curk, T.; Dobnikar, J.; Frenkel, D., Design principles for super selectivity using multivalent interactions. In *Multivalency*, Huskens, J., Prins, L. J., Haag, R., Ravoo, B. J., Eds. John Wiley & Sons Ltd.: 2017.
17. Zhang, K. Y. J.; Milburn, M. V.; Artis, D. R., Scaffold-Based Drug Discovery. In *Structure-Based Drug Discovery*, Springer Netherlands: Dordrecht, 2007; pp 129-153.
18. Welsch, M. E.; Snyder, S. A.; Stockwell, B. R. Privileged scaffolds for library design and drug discovery. *Current Opinion in Chemical Biology* **2010,** 14 (3), 347-361 DOI: https://doi.org/10.1016/j.cbpa.2010.02.018.
19. Lounnas, V.; Ritschel, T.; Kelder, J.; McGuire, R.; Bywater, R. P.; Foloppe, N. Current progress in structure-based rational drug design marks a new mindset in drug discovery. *Computational and Structural Biotechnology Journal* **2013,** 5 (6), e201302011 DOI: https://doi.org/10.5936/csbj.201302011.
20. Danial, M.; Root, M. J.; Klok, H.-A. Polyvalent side chain peptide–synthetic polymer conjugates as HIV-1 entry inhibitors. *Biomacromolecules* **2012,** 13 (5), 1438-1447 DOI: https://doi.org/10.1021/bm300150q.
21. Nwe, K.; Brechbiel, M. W. Growing Applications of "Click Chemistry" for Bioconjugation in Contemporary Biomedical Research. *Cancer Biotherapy and Radiopharmaceuticals* **2009,** 24 (3), 289-302 DOI: 10.1089/cbr.2008.0626.
22. Kolb, H. C.; Sharpless, K. B. The growing impact of click chemistry on drug discovery. *Drug Discovery Today* **2003,** 8 (24), 1128-1137 DOI: https://doi.org/10.1016/S1359-6446(03)02933-7.
23. Kolb, H. C.; Finn, M. G.; Sharpless, K. B. Click Chemistry: Diverse Chemical Function from a Few Good Reactions. *Angewandte Chemie International Edition* **2001,** 40 (11), 2004-2021 DOI: https://doi.org/10.1002/1521-3773(20010601)40:11%3C2004::AID-ANIE2004%3E3.0.CO;2-5.
24. Tasdelen, M. A. Diels–Alder "click" reactions: recent applications in polymer and material science. *Polymer Chemistry* **2011,** 2 (10), 2133-2145 DOI: 10.1039/C1PY00041A.
25. Hoyle, C. E.; Bowman, C. N. Thiol–Ene Click Chemistry. *Angewandte Chemie International Edition* **2010,** 49 (9), 1540-1573 DOI: 10.1002/anie.200903924.
26. Uygun, M.; Tasdelen, M. A.; Yagci, Y. Influence of Type of Initiation on Thiol–Ene "Click" Chemistry. *Macromolecular Chemistry and Physics* **2010,** 211 (1), 103-110 DOI: 10.1002/macp.200900442.

27. Hansell, C. F.; Espeel, P.; Stamenovic, M. M.; Barker, I. A.; Dove, A. P.; Du Prez, F. E.; O'Reilly, R. K. Additive-free clicking for polymer functionalization and coupling by tetrazine–norbornene chemistry. *Journal of the American Chemical Society* **2011,** 133 (35), 13828-13831 DOI: https://doi.org/10.1021/ja203957h.
28. Karver, M. R.; Weissleder, R.; Hilderbrand, S. A. Synthesis and evaluation of a series of 1, 2, 4, 5-tetrazines for bioorthogonal conjugation. *Bioconjugate chemistry* **2011,** 22 (11), 2263-2270 DOI: https://doi.org/10.1021/bc200295y.
29. Devaraj, N. K.; Weissleder, R.; Hilderbrand, S. A. Tetrazine-based cycloadditions: application to pretargeted live cell imaging. *Bioconjugate chemistry* **2008,** 19 (12), 2297-2299 DOI: https://doi.org/10.1021/bc8004446.
30. Agard, N. J.; Prescher, J. A.; Bertozzi, C. R. A Strain-Promoted [3 + 2] Azide−Alkyne Cycloaddition for Covalent Modification of Biomolecules in Living Systems. *Journal of the American Chemical Society* **2004,** 126 (46), 15046-15047 DOI: 10.1021/ja044996f.
31. Codelli, J. A.; Baskin, J. M.; Agard, N. J.; Bertozzi, C. R. Second-generation difluorinated cyclooctynes for copper-free click chemistry. *Journal of the American Chemical Society* **2008,** 130 (34), 11486-11493 DOI: 10.1021/ja803086r.
32. Debets, M. F.; van Berkel, S. S.; Schoffelen, S.; Rutjes, F. P. J. T.; van Hest, J. C. M.; van Delft, F. L. Aza-dibenzocyclooctynes for fast and efficient enzyme PEGylation via copper-free (3+2) cycloaddition. *Chemical Communications* **2010,** 46 (1), 97-99 DOI: 10.1039/B917797C.
33. Ning, X.; Guo, J.; Wolfert, M. A.; Boons, G.-J. Visualizing Metabolically Labeled Glycoconjugates of Living Cells by Copper-Free and Fast Huisgen Cycloadditions. *Angewandte Chemie International Edition* **2008,** 47 (12), 2253-2255 DOI: 10.1002/anie.200705456.
34. Mbua, N. E.; Guo, J.; Wolfert, M. A.; Steet, R.; Boons, G.-J. Strain-Promoted Alkyne–Azide Cycloadditions (SPAAC) Reveal New Features of Glycoconjugate Biosynthesis. *ChemBioChem* **2011,** 12 (12), 1912-1921 DOI: 10.1002/cbic.201100117.
35. Jewett, J. C.; Sletten, E. M.; Bertozzi, C. R. Rapid Cu-Free Click Chemistry with Readily Synthesized Biarylazacyclooctynones. *Journal of the American Chemical Society* **2010,** 132 (11), 3688-3690 DOI: 10.1021/ja100014q.
36. Debets, M. F.; van Berkel, S. S.; Dommerholt, J.; Dirks, A. J.; Rutjes, F. P. J. T.; van Delft, F. L. Bioconjugation with Strained Alkenes and Alkynes. *Accounts of Chemical Research* **2011,** 44 (9), 805-815 DOI: 10.1021/ar200059z.
37. Debets, M. F.; Prins, J. S.; Merkx, D.; van Berkel, S. S.; van Delft, F. L.; van Hest, J. C. M.; Rutjes, F. P. J. T. Synthesis of DIBAC analogues with excellent SPAAC rate constants. *Organic & Biomolecular Chemistry* **2014,** 12 (27), 5031-5037 DOI: https://doi.org/10.1039/C4OB00694A.
38. Dong, Z.-m.; Liu, X.-h.; Tang, X.-l.; Li, Y.-s. Synthesis of hyperbranched polymers with pendent norbornene functionalities via RAFT polymerization of a novel asymmetrical divinyl monomer. *Macromolecules* **2009,** 42 (13), 4596-4603 DOI: https://doi.org/10.1021/ma9005796.
39. Hansell, C. F.; O'Reilly, R. K. A "Mix-and-Click" Approach to Double Core–Shell Micelle Functionalization. *ACS Macro Letters* **2012,** 1 (7), 896-901 DOI: 10.1021/mz300230c.
40. Goldmann, A. S.; Glassner, M.; Inglis, A. J.; Barner-Kowollik, C. Post-Functionalization of Polymers via Orthogonal Ligation Chemistry. *Macromolecular rapid communications* **2013,** 34 (10), 810-849 DOI: https://doi.org/10.1002/marc.201300017.
41. Gauthier, M. A.; Gibson, M. I.; Klok, H. A. Synthesis of Functional Polymers by Post-Polymerization Modification. *Angewandte Chemie International Edition* **2009,** 48 (1), 48-58 DOI: https://doi.org/10.1002/anie.200801951.
42. Poloukhtine, A. A.; Mbua, N. E.; Wolfert, M. A.; Boons, G.-J.; Popik, V. V. Selective labeling of living cells by a photo-triggered click reaction. *Journal of the American Chemical Society* **2009,** 131 (43), 15769-15776 DOI: https://doi.org/10.1021/ja9054096.
43. Nainar, S.; Kubota, M.; McNitt, C.; Tran, C.; Popik, V. V.; Spitale, R. C. Temporal Labeling of Nascent RNA Using Photoclick Chemistry in Live Cells. *Journal of the American Chemical Society* **2017,** 139 (24), 8090-8093 DOI: 10.1021/jacs.7b03121.
44. Friscourt, F.; Ledin, P. A.; Mbua, N. E.; Flanagan-Steet, H. R.; Wolfert, M. A.; Steet, R.; Boons, G.-J. Polar dibenzocyclooctynes for selective labeling of extracellular glycoconjugates of living cells. *Journal of the American Chemical Society* **2012,** 134 (11), 5381-5389 DOI: https://doi.org/10.1021/ja3002666.
45. McNitt, C. D.; Cheng, H.; Ullrich, S.; Popik, V. V.; Bjerknes, M. Multiphoton Activation of Photo-Strain-Promoted Azide Alkyne Cycloaddition "Click" Reagents Enables in Situ Labeling with Submicrometer Resolution. *Journal of the American Chemical Society* **2017,** 139 (40), 14029-14032 DOI: 10.1021/jacs.7b08472.
46. Orski, S. V.; Poloukhtine, A. A.; Arumugam, S.; Mao, L.; Popik, V. V.; Locklin, J. High density orthogonal surface immobilization via photoactivated copper-free click chemistry. *Journal of the American Chemical Society* **2010,** 132 (32), 11024-11026 DOI: https://doi.org/10.1021/ja105066t.
47. Bjerknes, M.; Cheng, H.; McNitt, C. D.; Popik, V. V. Facile quenching and spatial patterning of cyclooctynes via strain-promoted alkyne–azide cycloaddition of inorganic azides. *Bioconjugate Chemistry* **2017,** 28, 1560-1565 DOI: https://doi.org/10.1021/acs.bioconjchem.7b00201.
48. Sun, P.; Yan, G.; Tang, Q.; Chen, Y.; Zhang, K. Well-defined cyclopropenone-masked dibenzocyclooctyne functionalized polymers from atom transfer radical polymerization. *Polymer* **2015,** 64, 202-209 DOI: https://doi.org/10.1016/j.polymer.2014.10.041.
49. Tang, Q.; Chen, J.; Zhao, Y.; Zhang, K. A ring-closure method for preparing cyclic polymers from unconjugated vinyl monomers. *Polymer Chemistry* **2015,** 6 (37), 6659-6663 DOI: https://doi.org/10.1039/C5PY01049G.
50. Qu, L.; Wu, Y.; Sun, P.; Zhang, K.; Liu, Z. Cyclopropenone-masked dibenzocyclooctyne end-functionalized polymers from reversible addition-fragmentation chain transfer polymerization. *Polymer* **2017,** 114, 36-43 DOI: http://dx.doi.org/10.1016/j.polymer.2017.02.071.
51. Sun, P.; Tang, Q.; Wang, Z.; Zhao, Y.; Zhang, K. Cyclic polymers based on UV-induced strain promoted azide-alkyne cycloaddition reaction. *Polymer Chemistry* **2015,** 6 (22), 4096-4101.
52. Chapman, R.; Gormley, A. J.; Stenzel, M. H.; Stevens, M. M. Combinatorial Low-Volume Synthesis of Well-Defined Polymers by Enzyme Degassing. *Angewandte Chemie International Edition* **2016,** 55 (14), 4500-4503 DOI: 10.1002/anie.201600112.
53. Gormley, A. J.; Chapman, R.; Stevens, M. M. Polymerization Amplified Detection for Nanoparticle-Based Biosensing. *Nano Letters* **2014,** 14 (11), 6368-6373 DOI: 10.1021/nl502840h.

54. Chapman, R.; Gormley, A. J.; Herpoldt, K.-L.; Stevens, M. M. Highly Controlled Open Vessel RAFT Polymerizations by Enzyme Degassing. *Macromolecules* **2014,** 47 (24), 8541-8547 DOI: 10.1021/ma5021209.
55. Yeow, J.; Chapman, R.; Gormley, A. J.; Boyer, C. Up in the air: oxygen tolerance in controlled/living radical polymerization. *Chemical Society Reviews* **2018,** 47, 4357-4387 DOI: https://doi.org/10.1039/C7CS00587C.
56. Oliver, S.; Zhao, L.; Gormley, A. J.; Chapman, R.; Boyer, C. Living in the Fast Lane—High Throughput Controlled/Living Radical Polymerization. *Macromolecules* **2019,** 52 (1), 3-23 DOI: 10.1021/acs.macromol.8b01864.
57. Gormley, A. J.; Yeow, J.; Ng, G.; Conway, Ó.; Boyer, C.; Chapman, R. An Oxygen-Tolerant PET-RAFT Polymerization for Screening Structure–Activity Relationships. *Angewandte Chemie* **2018,** 130, 1573-1578 DOI: https://doi.org/10.1002/anie.201711044.
58. Ng, G.; Yeow, J.; Xu, J.; Boyer, C. Application of oxygen tolerant PET-RAFT to polymerization-induced self-assembly. *Polymer Chemistry* **2017,** 8 (18), 2841-2851 DOI: 10.1039/C7PY00442G.
59. Corrigan, N.; Rosli, D.; Jones, J. W. J.; Xu, J.; Boyer, C. Oxygen Tolerance in Living Radical Polymerization: Investigation of Mechanism and Implementation in Continuous Flow Polymerization. *Macromolecules* **2016,** 49 (18), 6779-6789 DOI: https://doi.org/10.1021/acs.macromol.6b01306.
60. Xu, J.; Jung, K.; Boyer, C. Oxygen Tolerance Study of Photoinduced Electron Transfer–Reversible Addition–Fragmentation Chain Transfer (PET-RAFT) Polymerization Mediated by Ru(bpy)3Cl2. *Macromolecules* **2014,** 47 (13), 4217-4229 DOI: 10.1021/ma500883y.
61. Yeow, J.; Chapman, R.; Xu, J.; Boyer, C. Oxygen tolerant photopolymerization for ultralow volumes. *Polymer Chemistry* **2017,** 8, 5012-5022 DOI: 10.1039/C7PY00007C.
62. Xu, J.; Jung, K.; Atme, A.; Shanmugam, S.; Boyer, C. A Robust and Versatile Photoinduced Living Polymerization of Conjugated and Unconjugated Monomers and Its Oxygen Tolerance. *Journal of the American Chemical Society* **2014,** 136 (14), 5508-5519 DOI: 10.1021/ja501745g.
63. Li, B.; Russell, S. J.; Compaan, D. M.; Totpal, K.; Marsters, S. A.; Ashkenazi, A.; Cochran, A. G.; Hymowitz, S. G.; Sidhu, S. S. Activation of the proapoptotic death receptor DR5 by oligomeric peptide and antibody agonists. *Journal of Molecular Biology* **2006,** 361 (3), 522-536.
64. Saito, A.; Suzuki, Y.; Ogata, S.-i.; Ohtsuki, C.; Tanihara, M. Activation of osteo-progenitor cells by a novel synthetic peptide derived from the bone morphogenetic protein-2 knuckle epitope. *Biochimica et Biophysica Acta (BBA)-Proteins and Proteomics* **2003,** 1651 (1), 60-67.
65. D'Andrea, L. D.; Iaccarino, G.; Fattorusso, R.; Sorriento, D.; Carannante, C.; Capasso, D.; Trimarco, B.; Pedone, C. Targeting angiogenesis: structural characterization and biological properties of a de novo engineered VEGF mimicking peptide. *Proceedings of the National Academy of Sciences* **2005,** 102 (40), 14215-14220.
66. Yeow, J.; Joshi, S.; Chapman, R.; Boyer, C. A. J. M. A Self-Reporting Photocatalyst for Online Fluorescence Monitoring of High Throughput RAFT Polymerization. *Angewandte Chemie International Edition* **2018,** 57, 10102-10106 DOI: https://doi.org/10.1002/anie.201802992.
67. Werlang, C.; Cárcarmo-Oyarce, G.; Ribbeck, K. Engineering mucus to study and influence the microbiome. *Nature Reviews Materials* **2019,** 4 (2), 134-145 DOI: 10.1038/s41578-018-0079-7.
68. Kramer, J. J.; Nieger, M.; Bräse, S. Synthesis of Planar Chiral N-Heterocyclic-Substituted Pyridinophanes. *European Journal of Organic Chemistry* **2013,** 2013 (3), 541-549 DOI: https://doi.org/10.1002/ejoc.201201286.

Peer reviewed version of the manuscript published in final form in the Journal of the American Chemical Society, 2019, DOI: 10.1021/jacs.9b09899

FIGURES

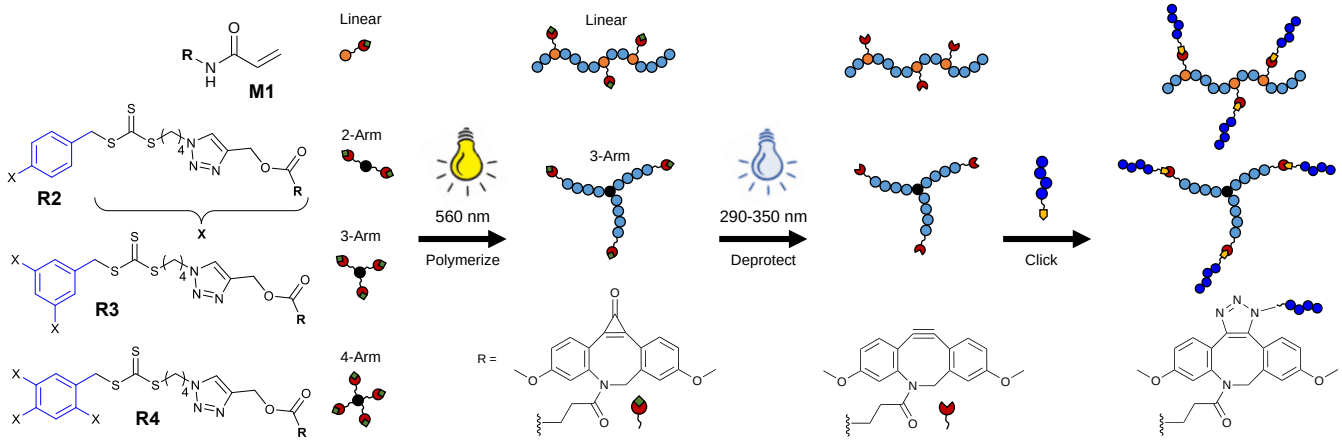

Figure 1. Reaction schematic. Cyclopropenone-masked DIBAC (cp-DIBAC) was synthesized either as a monomer (**M1**) or at the end of 2-arm (**R2**), 3-arm (**R3**), or 4-arm (**R4**) RAFT agents. Polymerization by PET-RAFT with 560 nm light followed by cp deprotection with UV produced SPAAC-ready polymer scaffolds for ligand clicking.

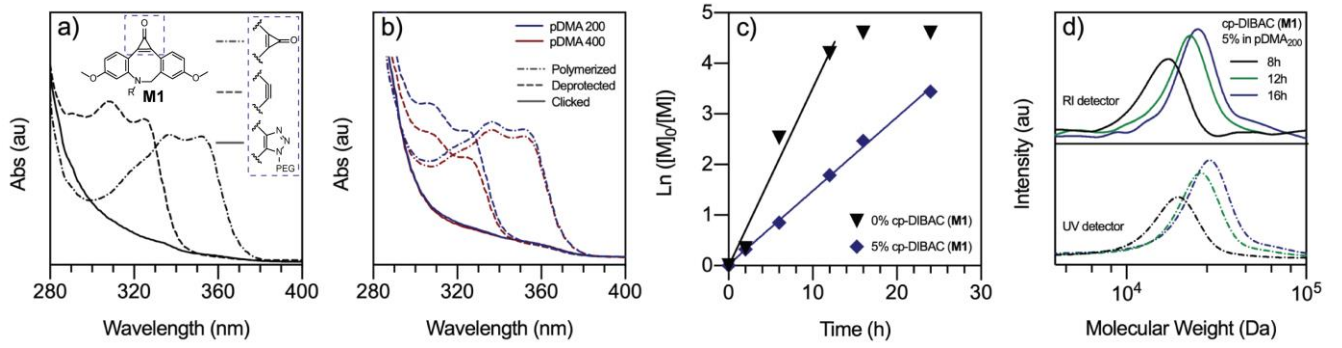

Figure 2. UV-Vis of cp-DIBAC and polymerization kinetics. a) UV-Vis of cp-DIBAC monomer (**M1**) before and after deprotection showing blue-shift of the characteristic peak, followed by a loss in absorbance after click to 2kDa PEG-N_3. b) UV-Vis traces of pDMA with 5% (mol) cp-DIBAC monomer (**M1**) incorporated at DP 200 and 400 before and after deprotection, and following click to 2kDa PEG-N_3. c) Kinetics of PET-RAFT polymerization with and without cp-DIBAC monomer (**M1**) showing complete conversion in both cases after 16h**.** d)∫ GPC traces for pDMA with 5% (mol) cp-DIBAC monomer (**M1**) after 8, 12 and 16h of polymerization, showing incorporation of the cp-DIBAC by UV detection at 265 nm.

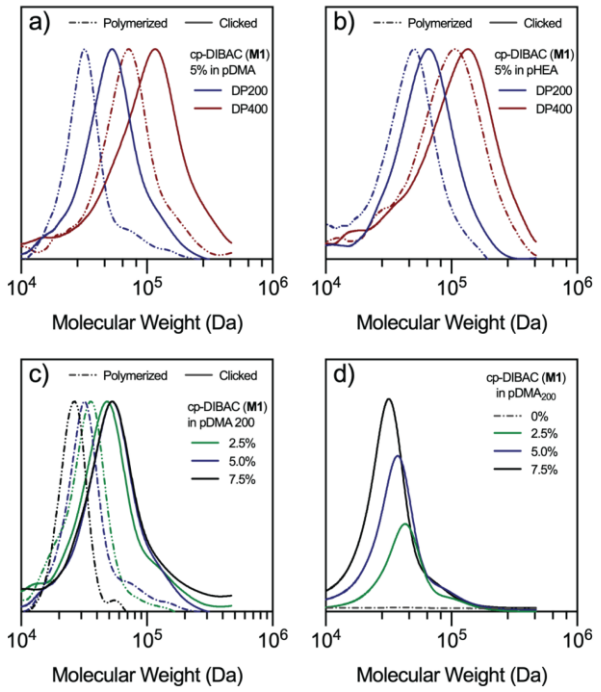

Figure 3. GPC traces showing the copolymerization of cp-DIBAC monomer (1) into side-chain functionalized linear polymers followed by click with 2kDa PEG-N_3. a) DMA with 5% cp-DIBAC, b) HEA with 5% cp-DIBAC, and c) DMA DP 200 with 2.5 – 7.5% cp-DIBAC. d) UV signal at 265 nm from GPC showing increasing incorporation of cp-DIBAC as a function of feed ratio.

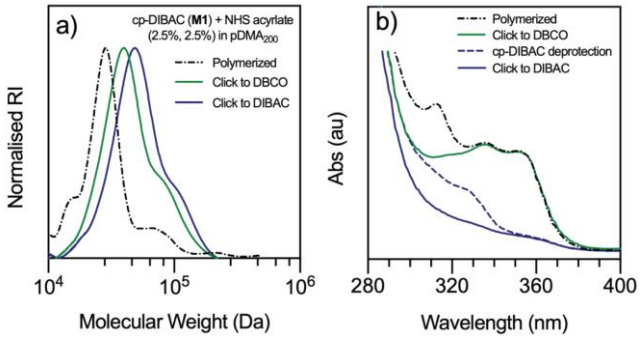

Figure 4. Dual functionalization by SPAAC. a) GPC traces after copolymerization of DMA / NHS-acrylate / cp-DIBAC (95 / 2.5 / 2.5 mol%) and addition of DBCO-NH_2 to create dual SPAAC-ready polymers. Subsequent click to DBCO, deprotection and secondary click of 2kDa PEG-N_3 to cp-DIBAC are shown in the green and blue lines respectively. b) UV-Vis traces of the protected polymer before and after the first DBCO click, after deprotection of the cp-DIBAC and after subsequent click to the DIBAC.

Peer reviewed version of the manuscript published in final form in the Journal of the American Chemical Society, 2019, DOI: 10.1021/jacs.9b09899

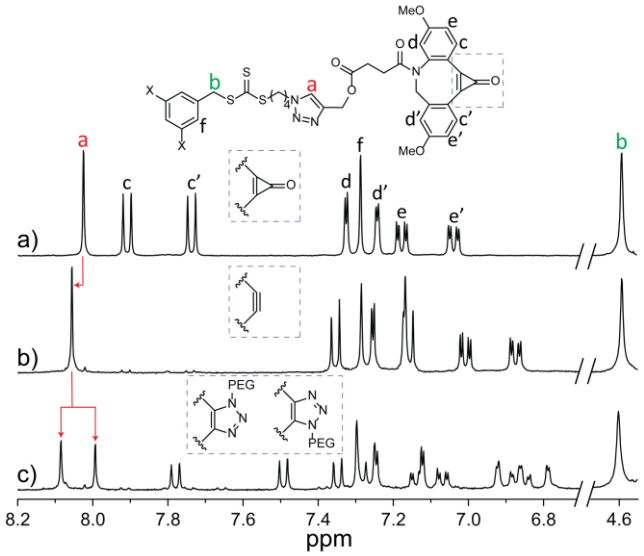

Figure 5. Deprotection and click of 3-arm star RAFT agent (3) by ^{1}H NMR (*d6*-DMSO). a) Before and b) after deprotection (3h UV) and c) after addition of 1.0 eq of 400 g.mol^{-1} PEG-N_3 with respect to DIBAC.

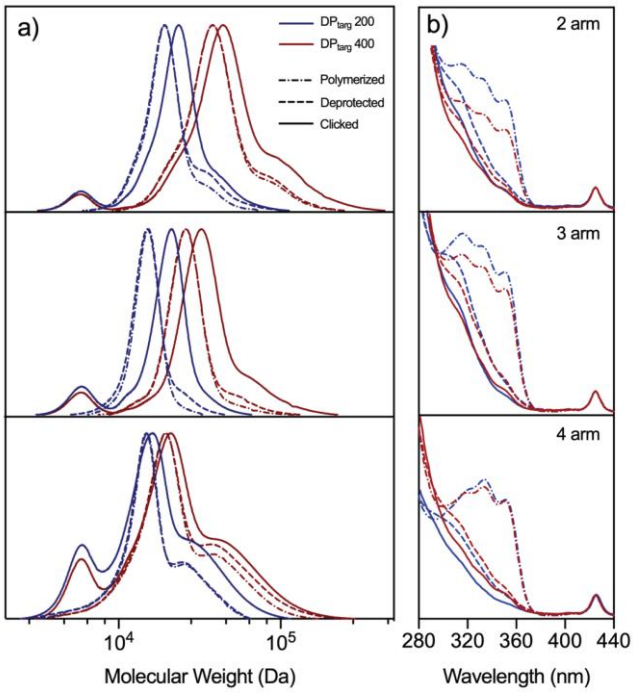

Figure 6. Polymerization, deprotection and SPAAC on star polymers. a) GPC and b) UV-Vis traces of DP$_{targ}$ 200 and 400 pDMA using 2 (top), 3 (middle) and 4 (bottom) armed RAFT agents before and after deprotection and after addition of 1.0 eq of 2kDa PEG-N_3 with respect to DIBAC.

Peer reviewed version of the manuscript published in final form in the Journal of the American Chemical Society, 2019, DOI: 10.1021/jacs.9b09899

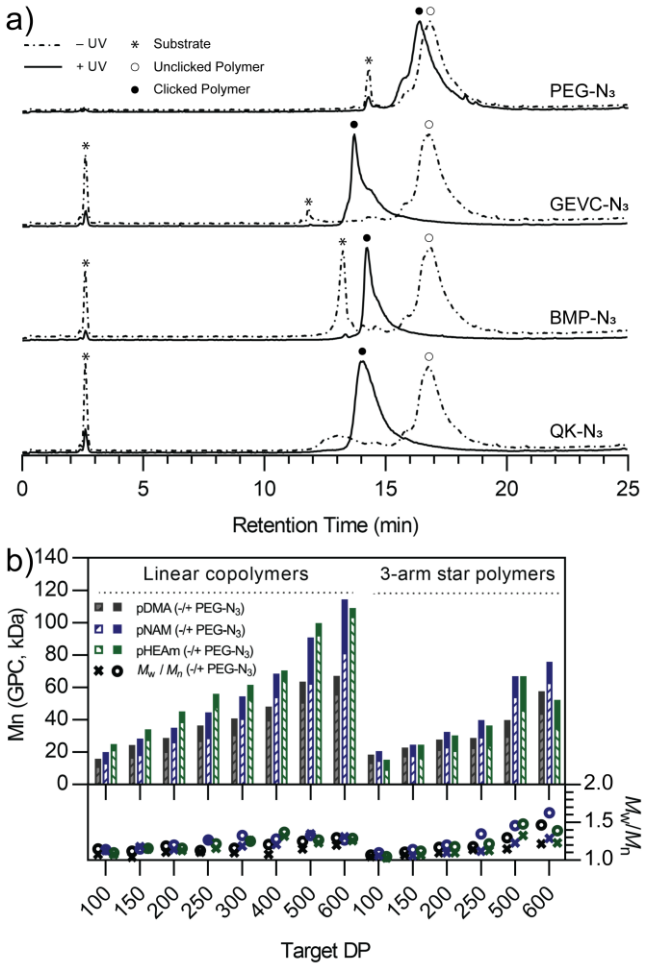

Figure 7. Scope of click and high throughput reactions a) Total positive ion count (TIC+) LC-MS data for mixtures of a 2-arm DP20 pDMA with 400 Da PEG-N_3 and three different peptides, with and without irradiation with UV light. Peaks corresponding to the polymer before (○) and after (●) click as well as the substrate peaks (*) are highlighted. b) Summary of GPC M_n and $Đ$ data high throughput polymer library of pDMA, pNAM and pHEAm linear copolymers (5% cp-DIBAC) and 3-arm star polymers before and after click with 2 kDa PEG-N_3. Full LC-MS data and GPC traces for each polymer are shown in the supporting information.

Peer reviewed version of the manuscript published in final form in the Journal of the American Chemical Society, 2019, DOI: 10.1021/jacs.9b09899

A Dual Wavelength Polymerization and Bioconjugation Strategy for High Throughput Synthesis of Multivalent Ligands

Zihao Li,[1‡] Shashank Kosuri,[2‡] Henry Foster,[1] Jarrod Cohen,[3] Coline Jumeaux,[4,5] Molly M. Stevens,[4,5] Robert Chapman,*[1] Adam J. Gormley*[2]

[1]Centre for Advanced Macromolecular Design (CAMD) and the Australian Centre for Nanotechnology (ACN), School of Chemistry, UNSW, Sydney, Australia

[2]Department of Biomedical Engineering, Rutgers, The State University of New Jersey, Piscataway, NJ 08854, USA

[3]New Jersey Center for Biomaterials, Rutgers, The State University of New Jersey, Piscataway, NJ 08854, USA

[4]Department of Materials, Department of Bioengineering, and the Institute for Biomedical Engineering, Imperial College London, London SW7 2AZ, United Kingdom

[5]Division of Medical Biochemistry and Biophysics (MBB), Karolinska Institutet, Stockholm, Sweden

SUPPORTING INFORMATION

1. Synthetic methods

Materials and instrumentation: All the raw materials for cp-DIBAC synthesis were purchased either from Sigma, VWR or Fisher Scientific and used as supplied. m-anisidine, m-anisaldehyde, Boc-Beta-Alanine-OH, aluminium chloride trace metal basis ($AlCl_3$) and triethylamine (TEA) were purchased from Sigma Aldrich, *N*-(3-dimethylaminopropyl)-*N′*-ethylcarbodiimide hydrochloride (EDC) from VWR international, hydroxybenzotriazole (HOBT) from Creosalus, and trifluoroacetic acid (TFA), acryloyl chloride and tetrachlorocyclopropene were purchased from Fisher scientific. Solvents DCM, hexane, ethyl acetate and methanol (MeOH) were purchased from VWR international and used as supplied. All other materials including the catalyst zinc tetraphenyl porphyrin (ZnTPP), the monomers and RAFT agent, and both the 2kDa and 400 Da azido-PEGs were purchased from Sigma-Aldrich and used as supplied.

^{1}H NMR spectra for monomer synthesis were obtained on a Varian VNMRS 500 MHz spectrometer and processed using Mestrenova 11.0.4. Molecular weights for linear polymers were determined using Agilent 1200 series GPC with differential refractive index (RI) detector and UV detector (265 nm) at 2 mg/mL concentration in DMF with 50 mM LiBr as the eluent. ^{1}H NMR spectra for star RAFT agent synthesis and star polymers were obtained with Bruker 300 MHz or 400 MHz spectrometers and processed using Topspin 3.6. The molecular weight distributions and molecular weights of star polymers were analysed via GPC with a Shimadzu modular system consisting three Phenomexex 5.0 µm bead-size columns (10^5, 10^4 and 10^3 Å) and RID-10A refractive index detector. DMF containing 0.1% LiBr and 0.04% 4-methoxyphenol was used as the mobile phase (flow rate = 1 mL·min^{-1}). The instrument was calibrated with commercially available linear PMMA standards (Polymer Laboratories).

LC-MS was run on a Shimadzu LCMS2020 using an analytical C18 column, and a gradient of 10-100% (v/v) MeCN in water over 26 min. 0.1% (v/v) formic acid was added to each eluent. Samples were prepared at ~0.1mg/ml in 1:1 MeCN/water (v/v) after removal of the DMSO in vacuo. 10 µL injections were used in each run, and the mass spectra (in positive and negative mode, m/z = 50-2000) and UV spectra (190-800 nm) were recorded as a function of time.

Peer reviewed version of the manuscript published in final form in the Journal of the American Chemical Society, 2019, DOI: 10.1021/jacs.9b09899

cp-DIBAC monomer synthesis procedure:

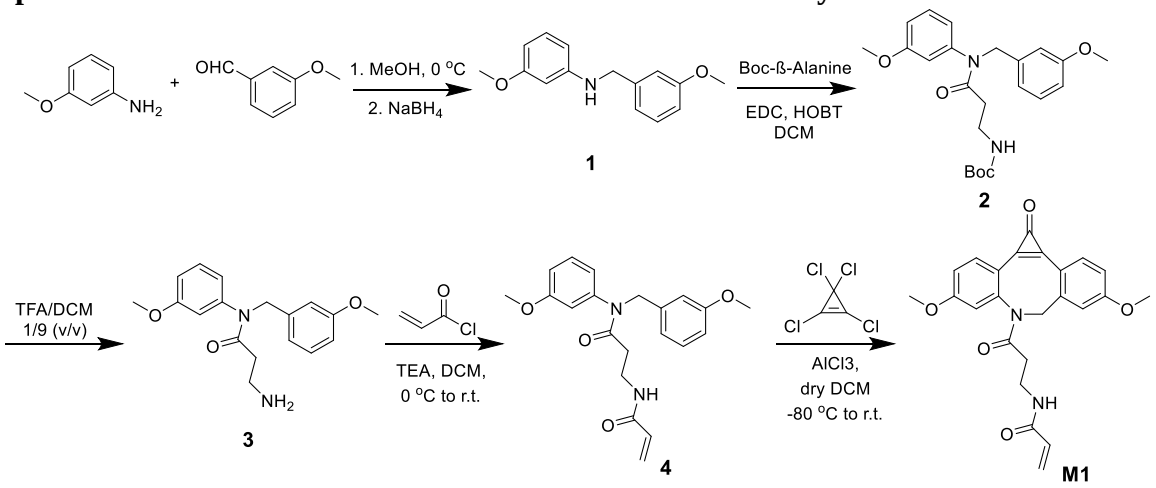

Scheme S1: Synthetic route of cp-DIBAC monomer M1

*Synthesis of **1**:* m-Anisidine (5 g, 40.6 mmol, 1.1 eq), m-anisaldehyde (5.02 g, 36.9 mmol, 1 eq), 100 mL methanol and a magnetic stir bar were added to a 250 mL round bottom flask (RBF) and allowed to mix for 2 h on an ice bath (0 °C). Sodium borohydride (4.2 g, 220, 3 eq) was added slowly for over a period of 1 h and the mixture was allowed to stir for an additional 2 h on ice prior to work up. 150 mL of deionized water (DI H_2O) was added slowly to quench the reaction causing a solid to form and precipitate out. The mixture was then extracted using ethyl acetate (3 x 100 mL) to separate the organic phase. Organic phases were then combined and washed with 0.5M HCl (2x 100 mL) to remove unreacted aniline followed by 2 M NaOH (2 x 100 mL), DI H_2O (2 x 50 mL), brine (1 x 100 mL) and finally dried over Na_2SO_4 for 10 minutes, filtered, and concentrated *in vacuo* to obtain a brown liquid. The liquid was air dried overnight to obtain the pure compound **1** (7.9 g, 80% yield). ^{1}H NMR (500 MHz, *d6*-DMSO) δ 7.28 – 7.16 (m, 1H), 6.91 (tdd, *J* = 7.5, 6.7, 5.6, 2.8 Hz, 3H), 6.80 – 6.73 (m, 1H), 6.24 – 6.13 (m, 2H), 6.13 –6.04 (m, 2H), 4.20 (dd, *J* = 6.2, 2.1 Hz, 2H), 3.70 (q, *J* = 2.7, 2.2 Hz, 3H), 3.61 (q, *J* = 2.0 Hz, 3H).

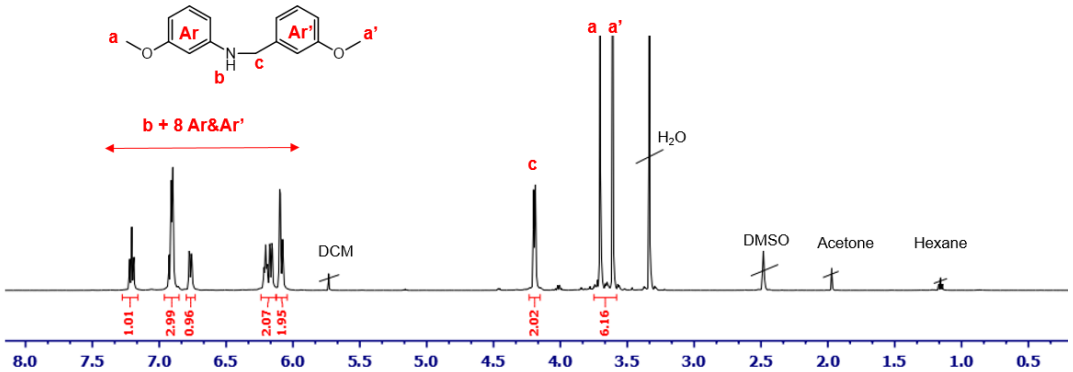

Figure S1: ^{1}H NMR (500 MHz *d6*-DMSO) of 1

*Synthesis of **2**:* Product **1** (4.5 g, 18.5 mmol, 1 eq) was mixed with Boc-Beta-alanine-OH (4.19 g, 22.14 mmol, 1.2 eq), EDC (4.97 g, 25.89 mmol, 1.4 eq), and HOBT (0.34 g, 2.2 mmol, 0.12 eq) in 100 mL DCM with a stir bar and allowed to mix for 30 h. The organic mixture was then washed with DI water (2 x 100 mL), 2 M NaOH (1 x 100 mL), DI water (1 x 100 mL) and finally with brine (1 x 100 mL) before being dried over Na_2SO_4 and concentrated *in vacuo*. The crude product was purified using column chromatography over silica (30:70 ethyl acetate: hexane) to yield the product as a brownish-red liquid **2** (3.44

g, 45%). ^{1}H NMR (500 MHz, *d6*-DMSO) δ 7.22 (dt, *J* = 35.0, 7.6 Hz, 2H), 6.88 (d, *J* = 8.2 Hz, 1H), 6.82 – 6.65 (m, 6H), 4.82 (s, 2H), 4.03 (t, *J* = 7.2 Hz, 1H), 3.70 (s, 6H), 3.41 (s, 1H), 2.28 (s, 2H), 1.34 (s, 9H).

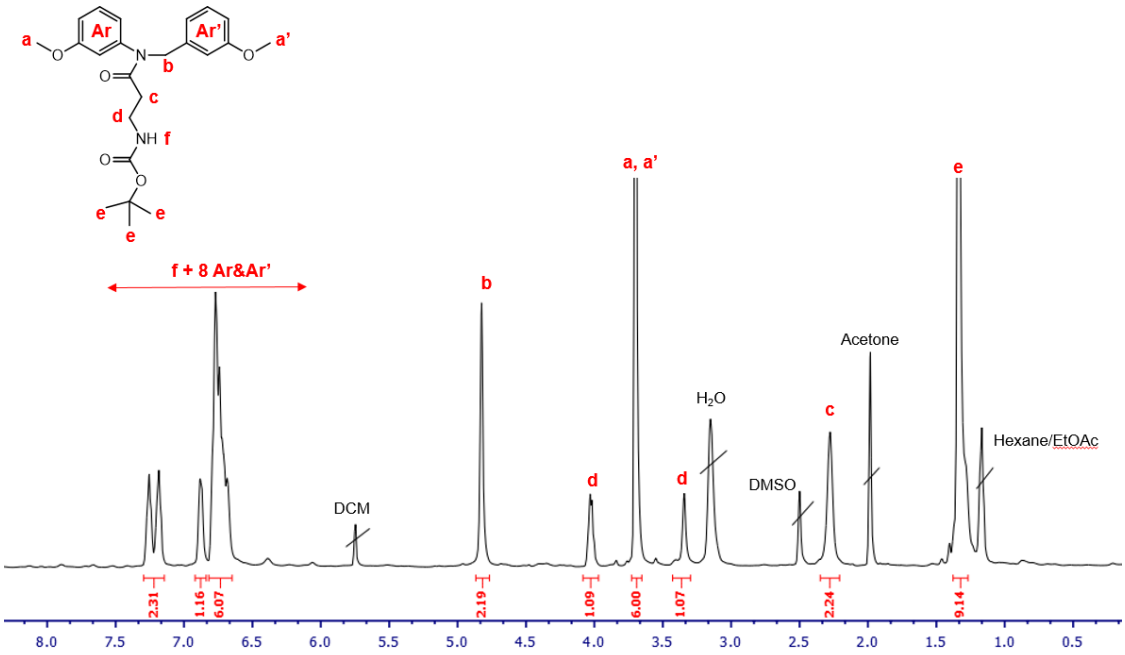

Figure S2: ^{1}H NMR (500 MHz *d6*-DMSO) of 2

*Synthesis of **3**:* Product **2** (3.44 g, 8.3 mmol) was dissolved in 50 mL of TFA and DCM (1:9, v:v) and allowed to stir for 4 h at room temperature for boc deprotection. The resulting solution was washed with 0.6 M $NaHCO_3$ (2 x 50 mL), DI water (1 x 50 mL) and finally with brine (1 x 50 mL) before being dried over Na_2SO_4 and concentrated *in vacuo* to yield the pure product as a dark pink liquid **3** (1.82 g, 70%). **Note:** Sodium bicarbonate wash is necessary to completely remove any TFA present even though this results in a decreased yield of product **3** because it will react with TEA in step 4 thereby affecting the stoichiometry. ^{1}H NMR (500 MHz, *d6*-DMSO) δ 7.26 (t, *J* = 8.1 Hz, 1H), 7.18 (t, *J* = 7.9 Hz, 1H), 6.89 – 6.84 (m, 1H), 6.79 – 6.68 (m, 5H), 4.80 (s, 2H), 3.68 (d, *J* = 5.6 Hz, 6H), 2.73 (t, *J* = 6.6 Hz, 2H), 2.21 (s, 2H).

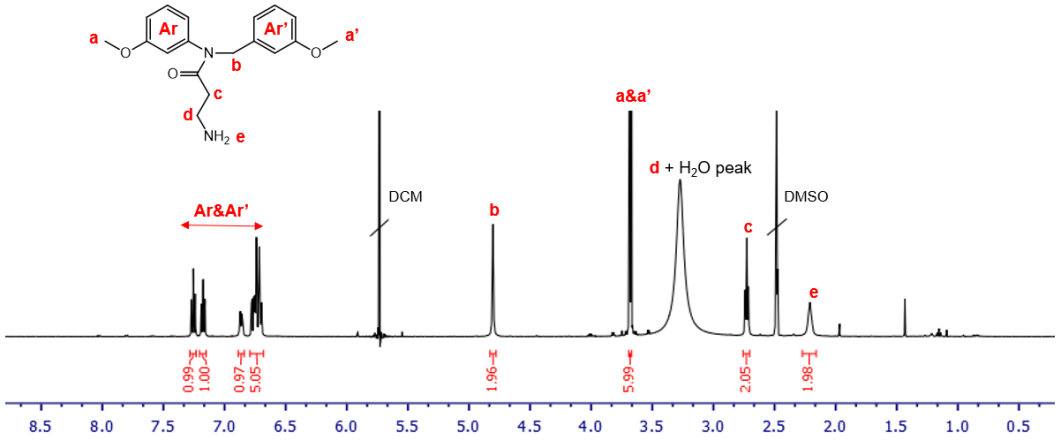

Figure S3: ^{1}H NMR (500 MHz *d6*-DMSO) of 3

*Synthesis of **4**:* Product **3** (1.82 g, 5.79 mmol, 1 eq) was mixed with 50 mL of DCM in a 100 mL RBF equipped with a magnetic stir bar and rubber septa and was placed on an ice bath at 0 °C. TEA (1.61 mL,

11.58 mmol, 2 eq) was added dropwise to the mixture using a syringe and was allowed to stir for half an hour at 0 °C. Acryloyl chloride (470 µL, 5.79 mmol, 1 eq) was then added dropwise carefully and the mixture was allowed to stir on the ice bath for an additional 2 h, cooled down to room temperature and continued stirring for additional 16 hrs before quenching it with 10 mL of methanol. Resulting solution was then washed with 0.1 M HCl (1 x 50 mL), DI water (2 x 50 mL) and finally with brine (1x 50 mL) before being dried over Na_2SO_4 and concentrated in vacuo. The crude was then purified with column chromatography over silica using 5% MeOH in DCM (v/v) to obtain the product 4 as a light pink liquid (1.109 g, 52%). ^{1}H NMR (500 MHz, *d6*-DMSO) δ 8.08 (s, 1H), 7.21 (dtd, *J* = 34.6, 8.0, 1.5 Hz, 2H), 6.90 – 6.83 (m, 1H), 6.79 – 6.66 (m, 5H), 6.15 (ddd, *J* = 17.1, 10.2, 1.5 Hz, 1H), 6.00 (dt, *J* = 17.2, 2.0 Hz, 1H), 5.51 (dt, *J* = 10.1, 1.9 Hz, 1H), 4.81 (s, 2H), 3.68 (d, *J* = 1.5 Hz, 6H), 2.30 (t, *J* = 7.0 Hz, 2H).

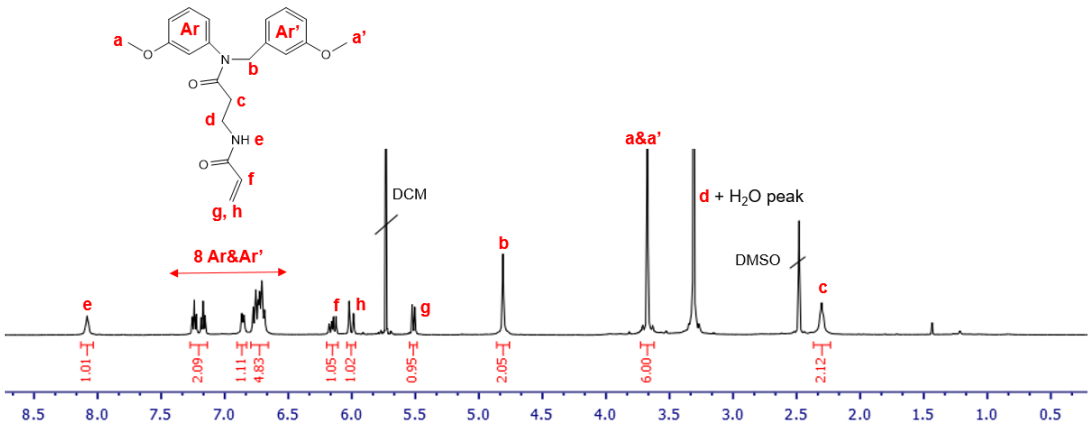

Figure S4: ^{1}H NMR (500 MHz *d6*-DMSO) of 4

*Synthesis of **M1**:* 50 mL of anhydrous DCM was added to a 100 mL flame dried two neck round bottom flask with a stir bar (one port with N_2 inlet and the other closed with a septum) and was cooled in an acetone-dry ice bath to -80 °C. The N_2 exhaust was removed after 10 min and $AlCl_3$ (1.60g, 12.04 mmol, 4 eq) was added very quickly and the inlet was closed once again. Tetrachlorocyclopropene (591 µL, 4.82 mmol, 1.6 eq) was added dropwise to the mixture through the septum via syringe-needle system and was allowed to stir for an hour at -80 °C. Product **4** (1.109 g, 3.01 mmol, 1 eq) was dissolved in 5 mL of anhydrous DCM and was added dropwise very slowly for over a period of one hour. After the addition of **4**, the reaction mixture was allowed to stir at -80 °C for another 2.5 h and later at room temperature overnight (16 h). The reaction was quenched by adding 10% HCl (10 mL) and was allowed to stir for another 5 min. The organic mixture was extracted with 50 mL of hexane and then washed with DI water (2 x 100 mL) and brine (1 x 50 mL) before being dried over Na_2SO_4 and concentrated *in vacuo*. The crude was purified by column chromatography over silica (10 % methanol in DCM v/v) to yield **M1** as a pale white solid (138 mg, 11%). ^{1}H NMR (500 MHz, *d6*-DMSO) δ 7.89 (d, *J* = 5.6 Hz, 2H), 7.74 (d, *J* = 7.8 Hz, 1H), 7.28 (d, *J* = 11.1 Hz, 2H), 7.17 (d, *J* = 8.5 Hz, 1H), 7.07 (d, *J* = 8.1 Hz, 1H), 6.06 – 5.89 (m, 2H), 5.48 (d, *J* = 9.6 Hz, 1H), 5.04 (d, *J* = 14.6 Hz, 1H), 4.23 (d, *J* = 14.8 Hz, 1H), 3.89 (s, 6H), 3.16 (s, 1H), 3.01 (s, 1H), 2.04 – 1.90 (m, 1H).

Peer reviewed version of the manuscript published in final form in the Journal of the American Chemical Society, 2019, DOI: 10.1021/jacs.9b09899

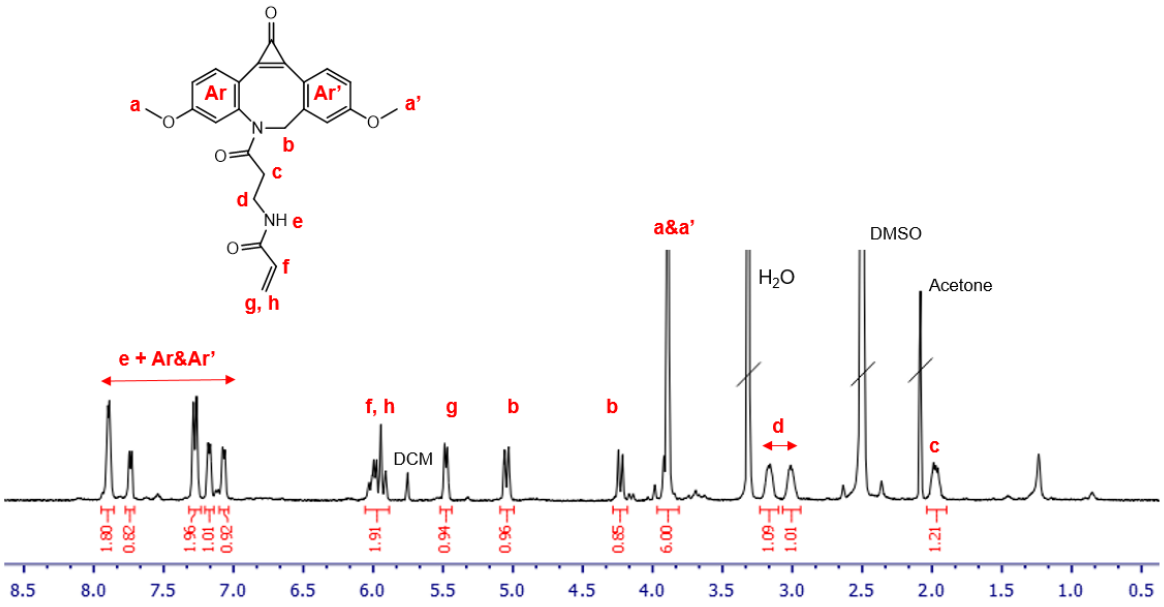

Figure S5: ^{1}H NMR (500 MHz *d6*-DMSO) of M1

Materials and instrumentation for star RAFT agent and polymer synthesis: ^{1}H NMR spectra were obtained on a Bruker 300 MHz or 400 MHz spectrometer and processed using Topspin 3.6.

The star polymers were characterised with a Shimadzu modular system consisting of DGU-12A degasser, LC-10AT pump, SIL-10AD auto-injector, CTO-10A column oven (50 °C), a guard column, three Phenomexex 5.0 µm bead-size columns (10^5, 10^4, and 10^3 Å) and RID-10A refractive index detector. Dimethylformamide (DMF) containing 0.1% LiBr and 0.04% 4-methoxyphenol was used as the mobile phase (flow rate = 1 mL·min^{-1}). Molecular weights are reported relative to commercially available linear PMMA standards (Polymer Laboratories) without Mark Houwink correction.

Peer reviewed version of the manuscript published in final form in the Journal of the American Chemical Society, 2019, DOI: 10.1021/jacs.9b09899

Star RAFT agent synthesis procedure:

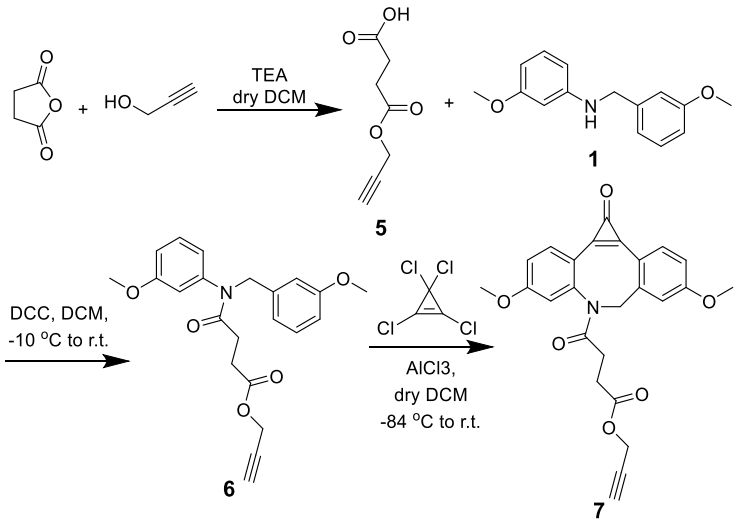

Scheme S2. Synthetic route of 7

*Synthesis of **5**:* A mixture of succinic anhydride (12.4 g, 124 mmol, 1.2 eq), propargyl alcohol (6.0 mL, 103 mmol, 1 eq) and triethylamine (15.7 mL, 113 mmol, 1.1 eq) were stirred overnight in anhydrous DCM (100 mL) in ambient temperature. The reaction mixture was quenched with 2 M HCl (50 mL). The aqueous layer was separated and extracted with DCM (2 × 50 mL). The combined organic solution was washed with DI water (100 mL) and brine (100 mL) before drying with $MgSO_4$ and concentrated with reduced pressure. The crude was purified by silica gel chromatography with EtOAc and hexane (1:1, v:v) to yield the product (11.6 g, 74.4 mmol, 72.1% yield). ^{1}H NMR (300 MHz, $CDCl_3$) δ 4.71 (d, J = 2.5 Hz, 1H, e), 2.77 – 2.62 (m, 2H, b&c), 2.48 (t, J = 2.5 Hz, 1H, g). ^{13}C NMR (76 MHz, $CDCl_3$) δ 177.40 (a), 171.48 (d), 77.51, (f), 75.22 (g), 52.47 (e), 28.76 (b&c).

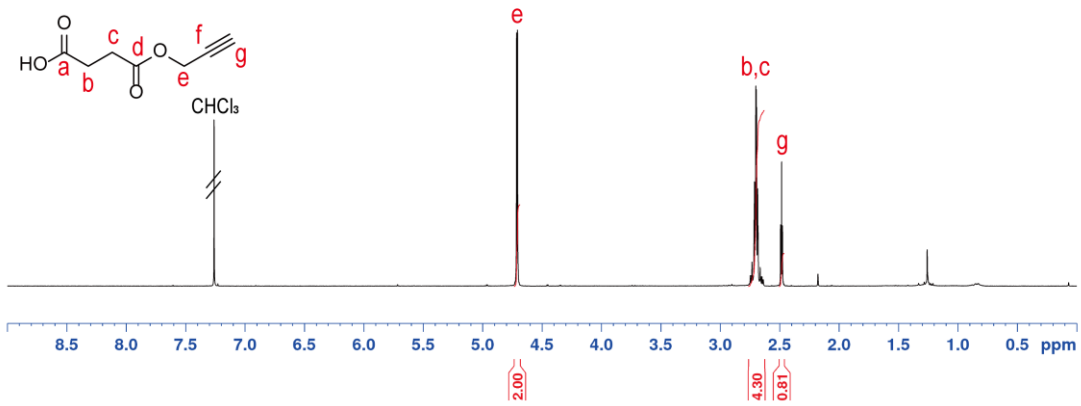

Figure S6. ^{1}H NMR (300 MHz, $CDCl_3$) of 5

*Synthesis of **6**:* A solution mixture of **1** (10.7 g, 44.4 mmol, 1 eq) and **5** (7.63 g, 48.9 mmol, 1.1 eq) in DCM (100 mL) was cooled to -10 °C in an ice/acetone bath. DCC (11.0 g, 53.3 mmol, 1.5 eq) was added in one portion and stirred at -10 °C for 1 h, then ambient temperature overnight. The white precipitate formed was filtered by silica and the solution mixture was diluted with DCM (200 mL). After washing with saturated $NaHCO_3$ (3000 mL), DI water (3000 mL) and brine (300 mL), the solution was dried with $MgSO_4$ and concentrated under vacuum. Purification of the crude by silica gel chromatography with EtOAc and hexane (1:2, v:v) yielded the product (14.8 g, 38.9 mmol, 87.6% yield). ^{1}H NMR (400 MHz, $CDCl_3$) δ 7.25 – 7.12 (m, 3H, Ar), 6.84 (dd, J = 8.3, 2.0 Hz, 1H, Ar), 6.81 – 6.73 (m, 3H, Ar), 6.65 (d, J

= 7.7 Hz, 1H, Ar), 6.57 (t, *J* = 1.9 Hz, 1H, Ar), 4.84 (s, *J* = 8.3 Hz, 2H, b), 4.68 (d, *J* = 2.5 Hz, 2H, d), 3.76 (s, 3H, c), 3.72 (s, 3H, c'), 2.69 (t, *J* = 6.6 Hz, 2H, e), 2.48 – 2.37 (m, 3H, f&g). ^{13}C NMR (101 MHz, $CDCl_3$) δ 172.36 (h), 171.13 (i), 160.51 (Ar), 159.77 (Ar), 143.25 (Ar), 139.15 (Ar), 130.40 (Ar), 129.45 (Ar), 121.17 (Ar), 120.78 (Ar), 114.28 (Ar), 114.08 (Ar), 113.87 (Ar), 113.27 (Ar), 77.84 (j), 74.94 (f), 55.48 (c), 55.35 (c'), 53.14 (b), 52.17 (d), 29.42 (e), 29.28 (g).

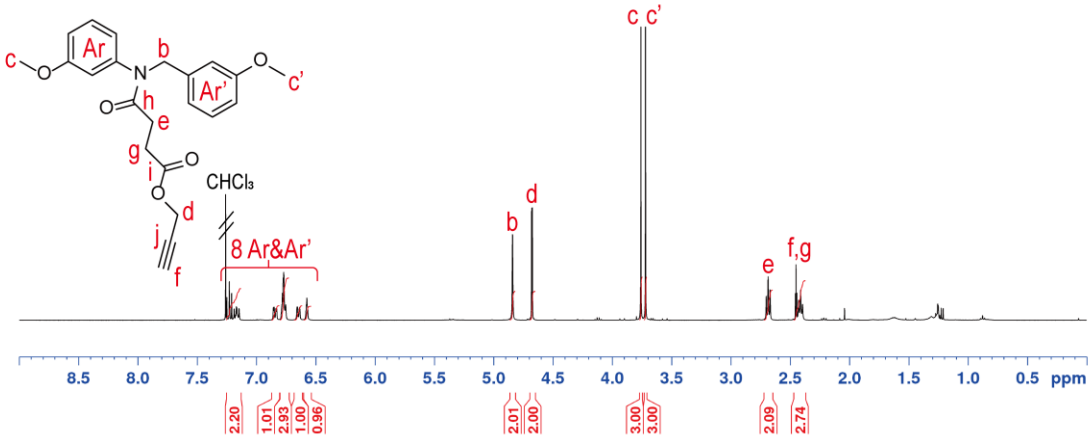

Figure S7. ^{1}H NMR (400 MHz, $CDCl_3$) of 6

Synthesis of ***7****.* A suspension of $AlCl_3$ (4.55 g, 34.1 mmol, 4 eq) in anhydrous DCM (70 mL) was cooled to -84 °C in a liquid N_2/EtOAc bath. Tetrachlorocyclopropene (1.67 mL, 13.6 mmol, 1.6 eq) was introduced into the mixture in one portion and stirred at -84 °C for 30 min. **6** (3.26 g, 8.55 mmol, 1 eq) was dissolved in anhydrous DCM (20 mL) and slowly added into the mixture over 1 h. The reaction mixture was kept at -84 °C under N_2 for another 1 h before stirring at ambient temperature overnight. After quenching the reaction with HCl (1 M, 70 mL), the separated aqueous layer was extracted with DCM (50 mL). The combined DCM solution was washed sequentially with DI water (150 mL × 3) and brine (150 mL) before drying with $MgSO_4$ and concentrated under reduced pressure. Gradient silica gel chromatography with EtOAc (70 to 100%) in hexane was performed to purify the product (1.10 g, 2.55 mmol, 29.9% yield). ^{1}H NMR (400 MHz, $CDCl_3$) δ 8.01 (d, *J* = 8.6 Hz, 1H, Ar), 7.90 (d, *J* = 8.5 Hz, 1H, Ar), 7.23 (d, *J* = 2.5 Hz, 1H, Ar), 7.15 (d, *J* = 2.5 Hz, 1H, Ar), 7.05 (dd, *J* = 8.6, 2.5 Hz, 1H, Ar), 6.95 (dd, *J* = 8.5, 2.6 Hz, 1H, Ar), 5.19 (d, *J* = 14.4 Hz, 1H, b_1), 4.72 – 4.60 (m, 1H, d_1), 4.51 (dd, *J* = 15.6, 2.5 Hz, 1H, d_2), 4.11 (d, *J* = 14.1 Hz, 1H, b_1), 3.93 (s, 3H, c), 3.90 (s, 3H, c'), 2.84 – 2.64 (m, 2H, e), 2.48 – 2.36 (m, 2H, f&g_1), 1.99 – 1.89 (m, 1H, g_2). ^{13}C NMR (101 MHz, $CDCl_3$) δ 172.03 (h), 171.82 (i), 163.28 (k), 162.82 (l), 152.71 (m), 145.94 (Ar), 143.38 (Ar), 141.64 (Ar), 139.11 (Ar), 136.03 (Ar), 135.29 (Ar), 118.24 (Ar), 115.75 (Ar), 115.54 (Ar), 115.19 (Ar), 114.47 (Ar), 113.83 (Ar), 77.62 (j), 75.13 (f), 56.40 (c), 56.13 (c'), 55.73 (b), 52.26 (d), 29.18 (e), 28.98 (g).

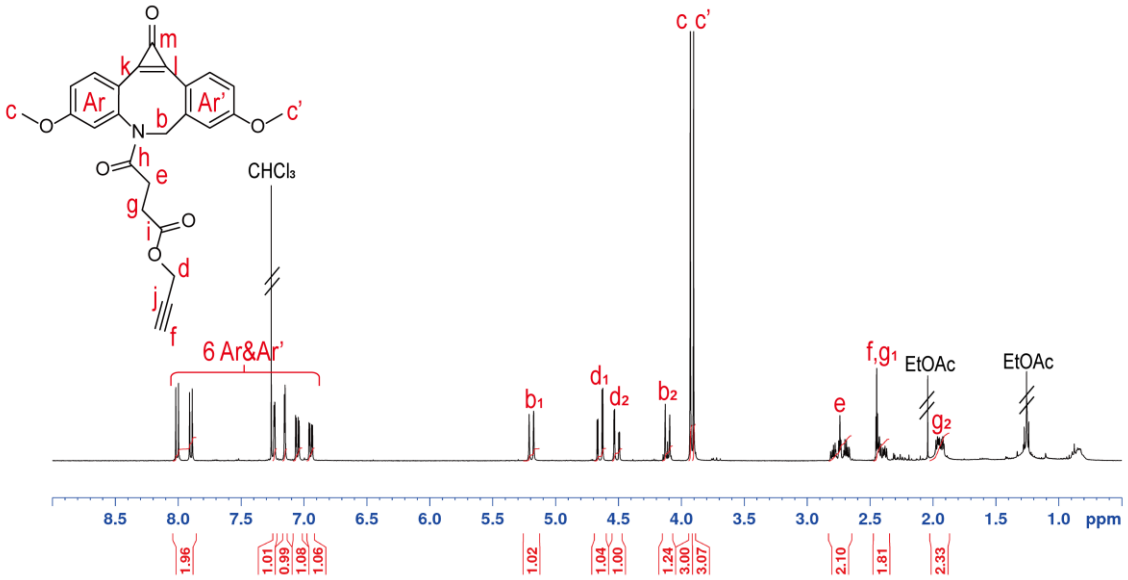

Figure S8.

^{1}H NMR (400 MHz, $CDCl_3$) of 7

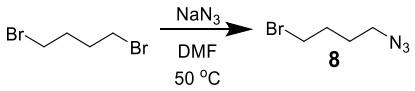

Scheme S3. Synthesis of 8

*Synthesis of **8***. A mixture of 1,4-dibromobutane (8.00 g, 37.0 mmol, 1.1 eq) and sodium azide (2.16 g, 33.3 mmol, 1 eq) in DMF (60 mL) was stirred at 50 °C overnight. After quenching the reaction with ice, the mixture was extracted with EtOAc (3 × 100 mL). The combined organic solution was washed with DI water (300 mL) and brine (300 mL), then dried with $MgSO_4$ and concentrated under vacuum. The crude was purified by gradient silica gel chromatography with EtOAc (0 to 5%) in hexane to obtain the product (1.63 g, 9.18 mmol, 24.8% yield). ^{1}H NMR (300 MHz, $CDCl_3$) δ 3.43 (t, J = 6.5 Hz, 2H, a), 3.33 (t, J = 6.6 Hz, 2H, d), 2.01 – 1.88 (m, 2H, b), 1.82 – 1.70 (m, 2H, c). ^{13}C NMR (76 MHz, $CDCl_3$) δ 50.73 (d), 32.99 (a), 29.90 (b), 27.61 (c).

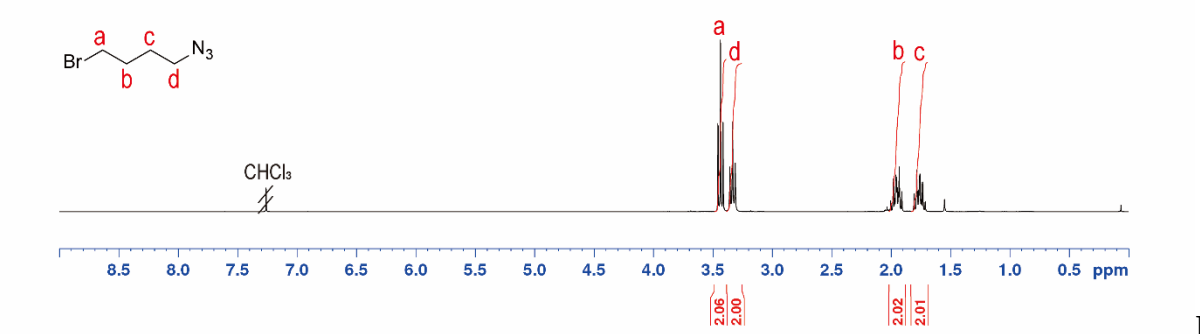

Figure S9.

^{1}H NMR (300 MHz, $CDCl_3$) of 8

Peer reviewed version of the manuscript published in final form in the Journal of the American Chemical Society, 2019, DOI: 10.1021/jacs.9b09899

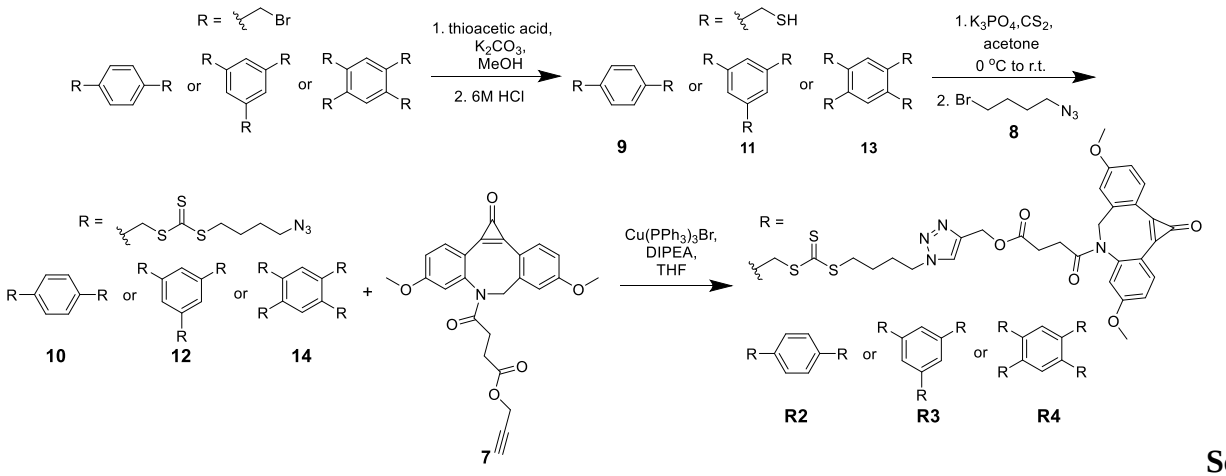

Scheme S4. Synthetic route of multiarmed RAFT agents

*Synthesis of **9***. **9** was synthesised by following a procedure adapted from a previous publication.[1] A suspension of 1,4-bis(bromomethyl)benzene (1.00 g, 3.81 mmol, 1 eq), thioacetic acid (650 µL, 9.10 mmol, 2.4 eq) and K_2CO_3 (1.26 g, 9.10 mmol, 2.4 eq) in MeOH (12 mL) was stirred at ambient temperature for 30 min. Another portion of K_2CO_3 (1.26 g, 9.10 mmol, 2.4 eq) was added and the mixture was stirred for 30 min before acidification with 6 M HCl to pH 4. The mixture was diluted with DI water (50 mL) and extracted with $CHCl_3$ (3 × 50 mL). The combined $CHCl_3$ layer was dried with $MgSO_4$, followed by the removal of solvent under reduced pressure to yield the product (659 mg, 3.87 mmol, quantitative yield). The product was used for later synthesis without further purification. ^{1}H NMR (400 MHz, $CDCl_3$) δ 7.28 (s, 3H, a), 3.73 (d, *J* = 7.5 Hz, 5H, b), 1.75 (t, *J* = 7.5 Hz, 2H, c).

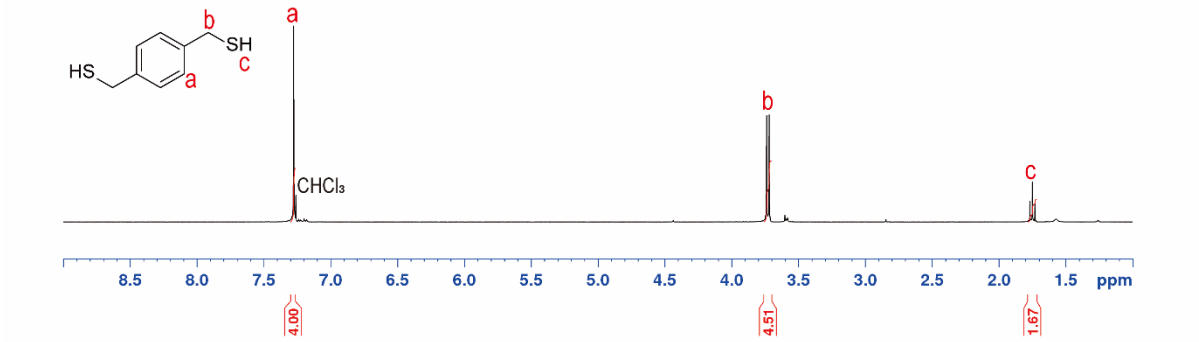

Figure S10. ^{1}H NMR (400 MHz, $CDCl_3$) of 9

*Synthesis of **10***. To an ice-bath-cooled suspension of **9** (734 mg, 4.31 mmol, 1 eq) and K_3PO_4 (1.83 g, 8.62 mmol, 2 eq) in acetone (35 mL) was added CS_2 (780 µL, 12.9 mmol, 3 eq) in one portion. The mixture was stirred in ambient temperature for 30 min and followed by the addition of **8** (1.69 g, 9.48 mmol, 2.2 eq) in one portion. The reaction mixture was stirred overnight and diluted with DCM (50 mL) before washing with 0.1 M HCl (2 × 50 mL), DI water (50 mL) and brine (50 mL). The organic solution was dried with $MgSO_4$ and concentrated under vacuum. Silica gel chromatography with EtOAc (10%) in hexane was performed to purify the product (1.44 g, 2.78 mmol, 64.4% yield). ^{1}H NMR (400 MHz, $CDCl_3$) δ 7.28 (s, 4H, a_1), 4.59 (s, 4H, b), 3.40 (t, *J* = 7.2 Hz, 4H, c), 3.32 (t, *J* = 6.6 Hz, 4H, f), 1.85 – 1.75 (m, 4H, d), 1.75 – 1.66 (m, 4H, e). ^{13}C NMR (76 MHz, $CDCl_3$) δ 134.85 (a_2), 129.69 (a_1), 50.98 (f), 41.04 (b), 36.31 (c), 28.16 (e), 25.60 (d).

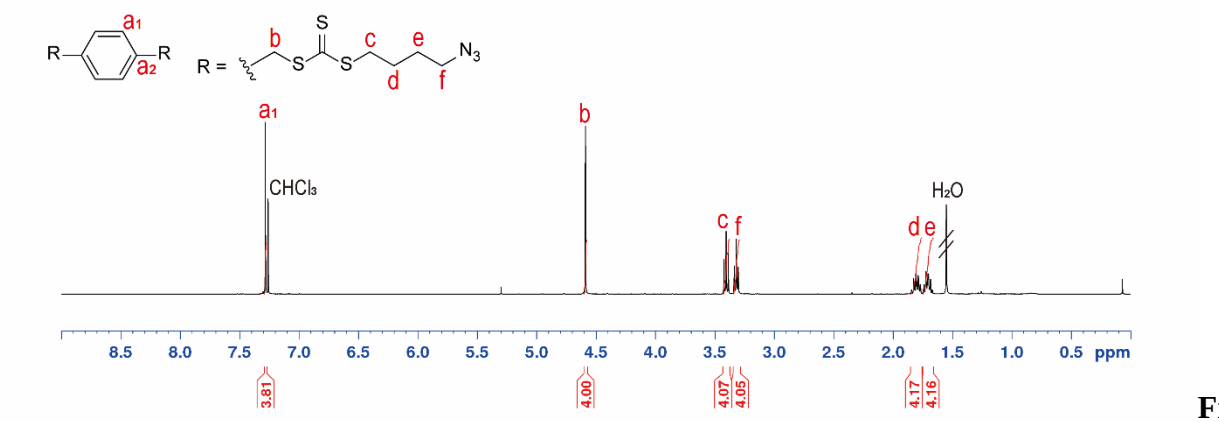

Figure S11. ^{1}H NMR (400 MHz, $CDCl_3$) of 10

*Synthesis of **R2***. A solution of **10** (27.2 mg, 52.7 µmol, 1 eq), **7** (50.0 mg, 116 µmol, 2.2 eq) and DIPEA (4.6 µL, 26.4 µmol, 0.5 eq) in THF was purged with nitrogen for 20 min. $Cu(PPh_3)_3Br$ (4.9 mg, 5.27 µmol, 0.1 eq) was suspended in THF (0.1 mL, purged with nitrogen) and added to the solution. The reaction mixture was purged with nitrogen for another 5 min, followed by stirring in ambient temperature under nitrogen for 2 days. The mixture was diluted with $CHCl_3$ (50 mL), washed with 0.1 M HCl (30 mL), DI water (30 mL) and brine (30 mL) and then dried with $MgSO_4$. The crude obtained after solvent evaporation was purified by gradient silica gel chromatography with MeOH (1 – 4%) in DCM to yield the product (43.5 mg, 31.5 µmol, 59.8% yield). ^{1}H NMR (400 MHz, *d6*-DMSO) δ 8.02 (s, 2H, Ar), 7.91 (d, *J* = 8.6 Hz, 2H, Ar), 7.74 (d, *J* = 8.4 Hz, 2H, Ar), 7.35 – 7.22 (m, 8H, Ar), 7.18 (dd, *J* = 8.6, 2.4 Hz, 2H, Ar), 7.05 (dd, *J* = 8.4, 2.5 Hz, 2H, Ar), 4.98 (m, 6H, b_1&d), 4.62 (s, 4H, k), 4.35 (t, *J* = 7.0 Hz, 4H, i), 4.23 (d, *J* = 14.3 Hz, 2H, b_2), 3.89 (s, 6H, c), 3.87 (s, 6H, c'), 3.39 (t, *J* = 7.3 Hz, 4H, j), 2.70 – 2.59 (m, 2H, e_1), 2.44 – 2.27 (m, 4H, f), 1.94 – 1.82 (m, 6H e_2&h), 1.66 – 1.55 (m, 4H, g). ^{13}C NMR (101 MHz, *d6*-DMSO) δ 171.84 (m), 170.87 (l), 162.65 (o), 161.80 (n), 151.07 (p), 145.71 (Ar), 142.57 (Ar), 142.27 (Ar), 141.70 (Ar), 139.34 (Ar), 134.93 (Ar), 134.70 (Ar), 134.38 (Ar), 129.47 (Ar), 124.52 (Ar), 118.46 (Ar), 115.57 (Ar), 115.36 (Ar), 114.67 (Ar), 114.49 (Ar), 113.09 (Ar), 57.18 (d), 56.07 (b), 55.83 (c), 55.67 (c'), 40.19 (k), 48.74 (i), 35.62 (j), 29.60 (e), 28.79 (f), 28.71 (h), 24.72 (g).

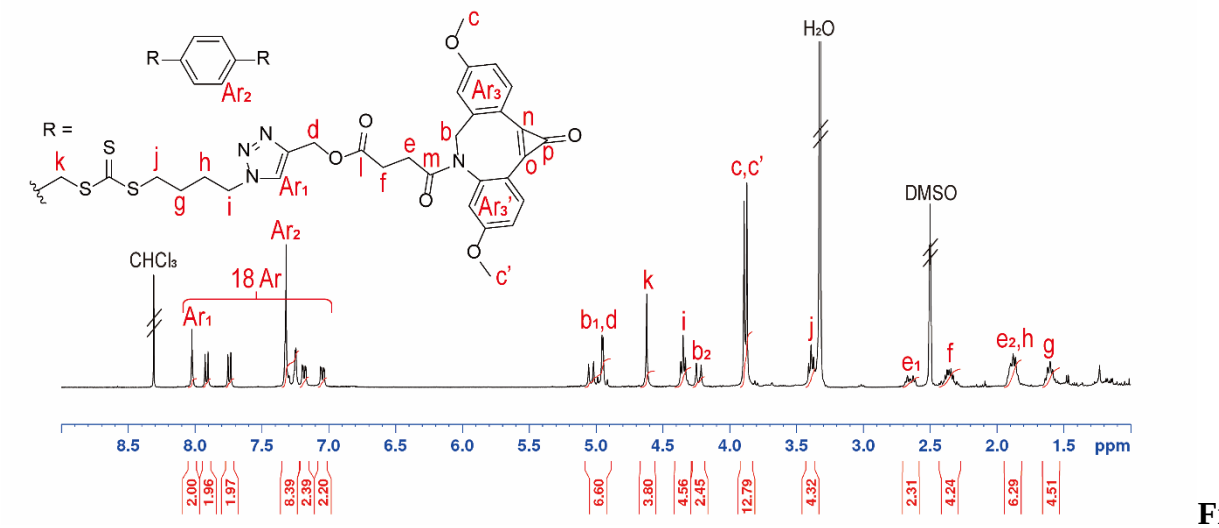

Figure S12. ^{1}H NMR (400 MHz, *d6*-DMSO) of R2

*Synthesis of **11***. **11** was synthesised and purified (94.8% yield) under the same conditions as for the synthesis of **9** while keeping ratio of number of arm : thioacetic acid : K_2CO_3 as 1 : 1.5 : 1.5. ^{1}H NMR (400 MHz, $CDCl_3$) δ 7.17 (s, *J* = 5.4 Hz, 3H, a), 3.72 (d, *J* = 7.6 Hz, 6H, b), 1.78 (t, *J* = 7.6 Hz, 3H, c).

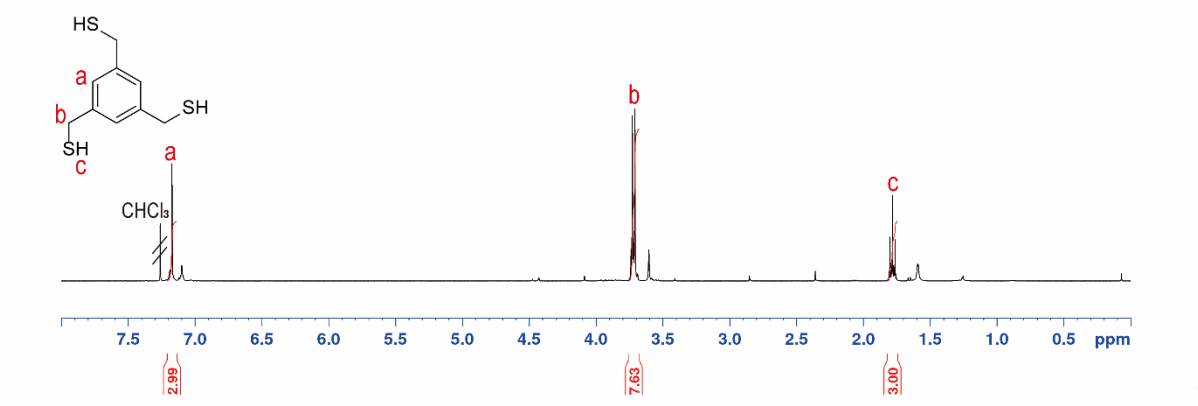

Figure S13. ^{1}H NMR (400 MHz, $CDCl_3$) of 11

*Synthesis of **12***. **12** was synthesised and purified (57.6% yield) under the same conditions as for the synthesis of **10** while keeping ratio of number of arm : K_3PO_4 : CS_2 : **8** as 1 : 1 : 1.5 : 1.2. ^{1}H NMR (400 MHz, $CDCl_3$) δ 7.21 (s, 3H, a_1), 4.55 (s, 6H, b), 3.41 (t, *J* = 7.2 Hz, 6H, c), 3.33 (t, *J* = 6.6 Hz, 6H, f), 1.86 – 1.75 (m, 6H, d), 1.76 – 1.66 (m, 6H, e). ^{13}C NMR (101 MHz, $CDCl_3$) δ 136.44 (a_2), 129.61 (a_1), 51.01 (f), 40.87 (b), 36.39 (c), 28.19 (e), 25.61 (d).

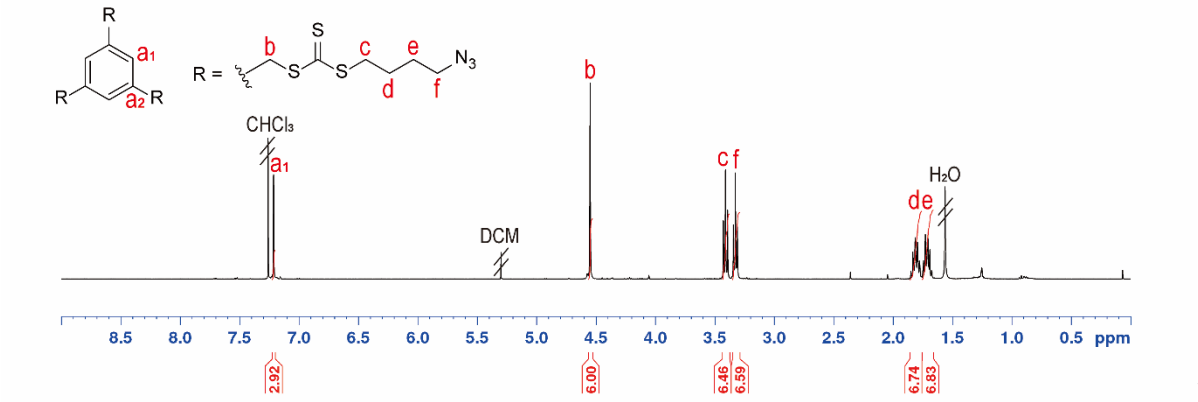

Figure S14. ^{1}H NMR (400 MHz, $CDCl_3$) of 12

*Synthesis of **R3***. **R3** was synthesised and purified (25.8% yield) under the same conditions as for the synthesis of **R2** while keeping ratio of number of arm : **7** : DIPEA : $Cu(PPh_3)_3Br$ as 1 : 1.1 : 0.25 : 0.05. ^{1}H NMR (400 MHz, *d6*-DMSO) δ 8.02 (s, 3H, Ar), 7.91 (d, *J* = 8.6 Hz, 3H, Ar), 7.74 (d, *J* = 8.5 Hz, 3H, Ar), 7.32 (d, *J* = 2.5 Hz, 3H, Ar), 7.29 (s, 3H, Ar), 7.24 (d, *J* = 2.5 Hz, 3H, Ar), 7.18 (dd, *J* = 8.6, 2.5 Hz, 3H, Ar), 7.04 (dd, *J* = 8.5, 2.6 Hz, 3H, Ar), 5.07 – 4.88 (m, 9H, b_1&d), 4.59 (s, 6H, k), 4.34 (t, *J* = 7.0 Hz, 6H, i), 4.23 (d, *J* = 14.5 Hz, 3H, b_2), 3.88 (s, 9H, c), 3.86 (s, 9H, c'), 3.38 (t, *J* = 7.3 Hz, 6H, j), 2.70 – 2.59 (m, 3H, e_1), 2.43 – 2.27 (m, 6H, f), 1.93 – 1.82 (m, 9H, e_2&h), 1.65 – 1.52 (m, 6H, g). ^{13}C NMR (101 MHz, *d6*-DMSO) δ 171.86 (m), 170.89 (l), 162.64 (o), 161.80 (n), 151.07 (p), 145.71 (Ar), 142.57 (Ar), 142.28 (Ar), 141.70 (Ar), 139.34 (Ar), 136.23 (Ar), 134.94 (Ar), 134.39 (Ar), 129.27 (Ar), 124.53 (Ar), 118.47 (Ar), 115.59 (Ar), 115.37 (Ar), 114.68 (Ar), 114.49 (Ar), 113.08 (Ar), 57.19 (d), 56.08 (b), 55.67 (c), 55.32 (c'), 40.19 (k), 48.76 (i), 35.69 (j), 28.86 (e), 28.81 (f), 28.71 (h), 24.72 (g).

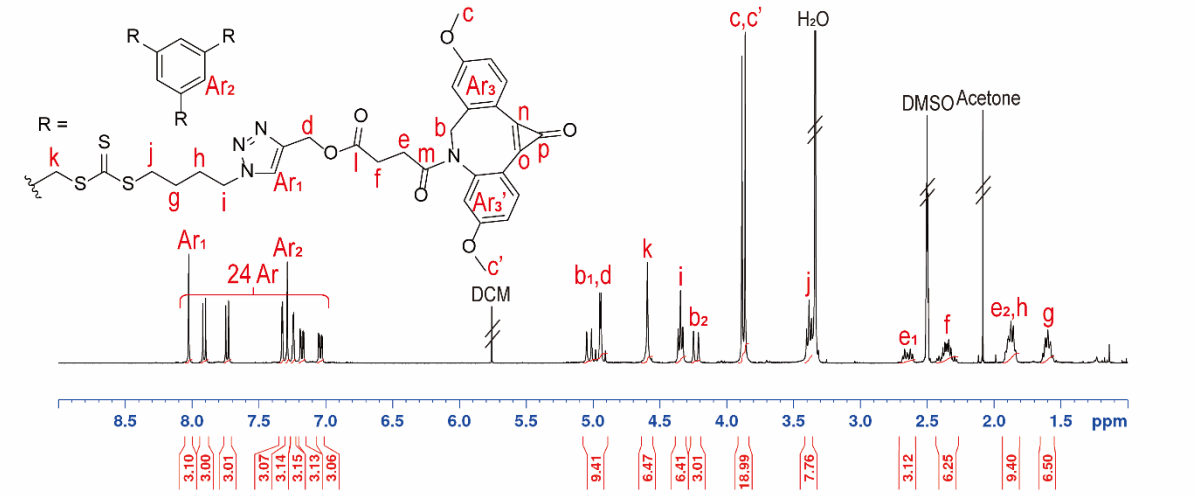

Figure S15. ^{1}H NMR (400 MHz, *d6*-DMSO) of R3

*Synthesis of **13***. **13** was synthesised and purified (quantitative yield) under the same conditions as for the synthesis of **9** while keeping ratio of number of arm : thioacetic acid : K_2CO_3 as 1 : 1.5 : 1.5. ^{1}H NMR (400 MHz, $CDCl_3$) δ 7.20 (s, 2H), 3.82 (d, *J* = 7.2 Hz, 8H), 1.86 (t, *J* = 7.2 Hz, 4H).

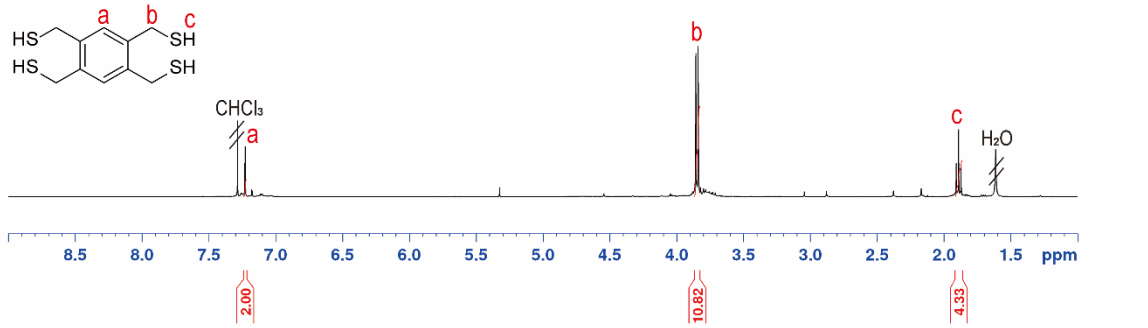

Figure S16. ^{1}H NMR (400 MHz, $CDCl_3$) of 13

*Synthesis of **14***. **14** was synthesised and purified (57.6% yield) under the same conditions as for the synthesis of **10** while keeping ratio of number of arm : K_3PO_4 : CS_2 : **8** as 1 : 1 : 1.5 : 1.2. ^{1}H NMR (400 MHz, $CDCl_3$) δ 7.36 (s, 2H, a_1), 4.61 (s, 8H, b), 3.41 (t, *J* = 7.2 Hz, 8H, c), 3.33 (t, *J* = 6.6 Hz, 8H, f), 1.86 – 1.76 (m, 8H, d), 1.76 – 1.66 (m, 8H, e). ^{13}C NMR (101 MHz, $CDCl_3$) δ 134.35 (a_2), 133.65 (a_1), 51.01 (f), 38.46 (b), 36.47 (c), 28.20 (e), 25.62 (d).

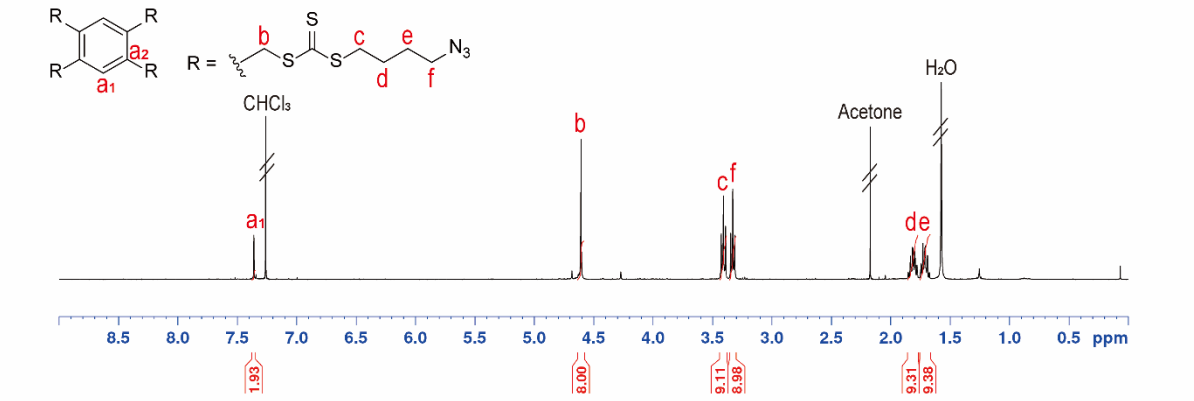

Figure S17. ^{1}H NMR (400 MHz, $CDCl_3$) of 14

*Synthesis of **R4***. **R4** was synthesised and purified (19.0% yield) under the same conditions as for the synthesis of **R2** while keeping ratio of number of arm : **7** : DIPEA : $Cu(PPh_3)_3Br$ as 1 : 1.1 : 0.25 : 0.05.

Peer reviewed version of the manuscript published in final form in the Journal of the American Chemical Society, 2019, DOI: 10.1021/jacs.9b09899

^{1}H NMR (400 MHz, *d6*-DMSO) δ 8.02 (s, 4H, Ar), 7.90 (d, *J* = 8.6 Hz, 4H, Ar), 7.73 (d, *J* = 8.5 Hz, 4H, Ar), 7.47 (s, 2H, Ar), 7.32 (d, *J* = 2.4 Hz, 4H, Ar), 7.23 (d, *J* = 2.5 Hz, 4H, Ar), 7.17 (dd, *J* = 8.6, 2.5 Hz, 4H, Ar), 7.03 (dd, *J* = 8.5, 2.6 Hz, 4H, Ar), 4.97 (dt, *J* = 16.3, 13.7 Hz, 12H, b_1&d), 4.65 (s, 8H, k), 4.34 (t, *J* = 7.0 Hz, 8H, i), 4.22 (d, *J* = 14.5 Hz, 4H, , b_2), 3.88 (s, 12H, c), 3.85 (s, 12H, c'), 3.38 (t, *J* = 7.3 Hz, 8H, j), 2.69 – 2.59 (m, 4H, e_1), 2.43 – 2.26 (m, 8H, f), 1.94 – 1.81 (m, 12H, e_2&h), 1.66 – 1.54 (m, 8H, g). ^{13}C NMR (101 MHz, *d6*-DMSO) δ 171.86 (m), 170.89 (l), 162.64 (o), 161.80 (n), 151.07 (p), 145.70 (Ar), 142.57 (Ar), 142.27 (Ar), 141.71 (Ar), 139.34 (Ar), 134.94 (Ar), 134.39 (Ar), 133.92 (Ar), 130.44 (Ar), 124.52 (Ar), 118.46 (Ar), 115.58 (Ar), 115.36 (Ar), 114.67 (Ar), 114.48 (Ar), 113.07 (Ar), 57.19 (d), 56.07 (b), 55.66 (c), 55.32 (c'), 48.76 (i), 37.53 (k), 35.77 (i), 28.87 (e), 28.81 (f), 28.71 (h), 24.73 (g).

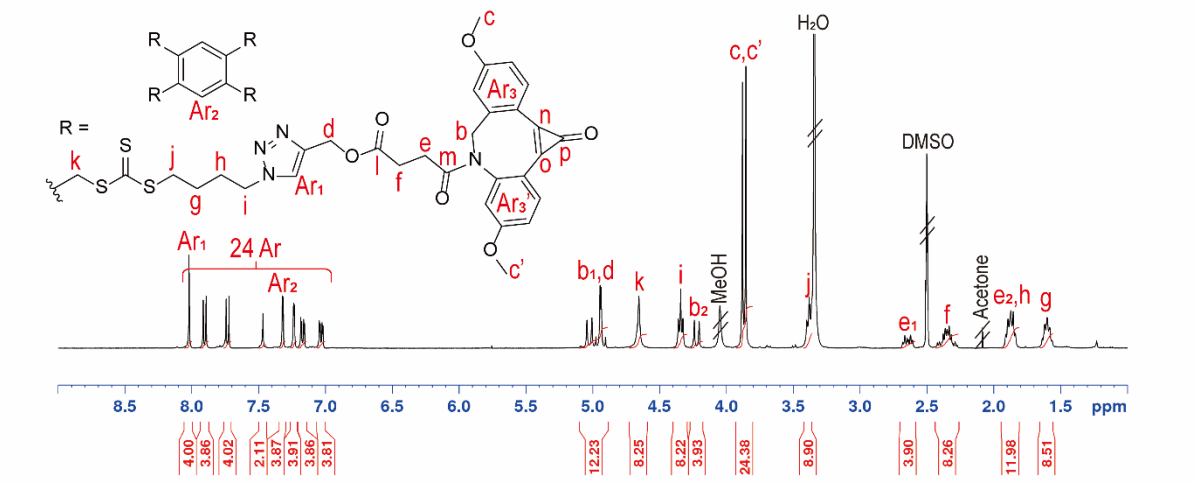

Figure S18. ^{1}H NMR (400 MHz, *d6*-DMSO) of R4

Peer reviewed version of the manuscript published in final form in the Journal of the American Chemical Society, 2019, DOI: 10.1021/jacs.9b09899

2. Additional figures and tables

Table S1: ^{1}H NMR and GPC results of cp-DIBAC copolymerized linear polymers before and after clicking

#	Monomer	DP_{targ} (total)	% (mol) **1**	X (%)	Polymerized			Clicked	
					$M_{n,theo}$	$M_{n,GPC}$	Đ	$M_{n,GPC}$	Đ
1	DMA	200	2.5	98	21.9	27.7	1.15	37.7	1.29
2	DMA	200	5	95	23.5	29.1	1.15	41.7	1.30
3	DMA	200	7.5	91	25.3	23.6	1.11	46.1	1.26
4	DMA	400	5	92	46.7	55.1	1.27	82.1	1.34
5	HEA	200	5	93	26.6	40.4	1.27	51.2	1.26
6	HEA	400	5	89	52.9	70.6	1.44	94.3	1.35

Table S2. ^{1}H NMR and GPC results of polymerized, deprotected and click on star polymers

#	CTA	DPtarg (total)	X (%)	Polymerized			Deprotected		Clicked	
				$M_{n,theo}$	$M_{n,GPC}$	Đ	$M_{n,GPC}$	Đ	$M_{n,GPC}$	Đ
1	2	200	61	13.4	17.8	1.16	18.2	1.13	21.6	1.12
2	2	400	63	27.0	32.1	1.22	32.5	1.23	38.4	1.34
3	3	200	55	13.5	14.4	1.04	14.3	1.07	19.4	1.07
4	3	400	63	27.7	23.7	1.10	23.9	1.12	30.1	1.19
5	4	200	94	21.2	14.1	1.19	13.9	1.21	17.1	1.18
6	4	400	74	32.0	17.6	1.33	18.0	1.40	21.3	1.31

Peer reviewed version of the manuscript published in final form in the Journal of the American Chemical Society, 2019, DOI: 10.1021/jacs.9b09899

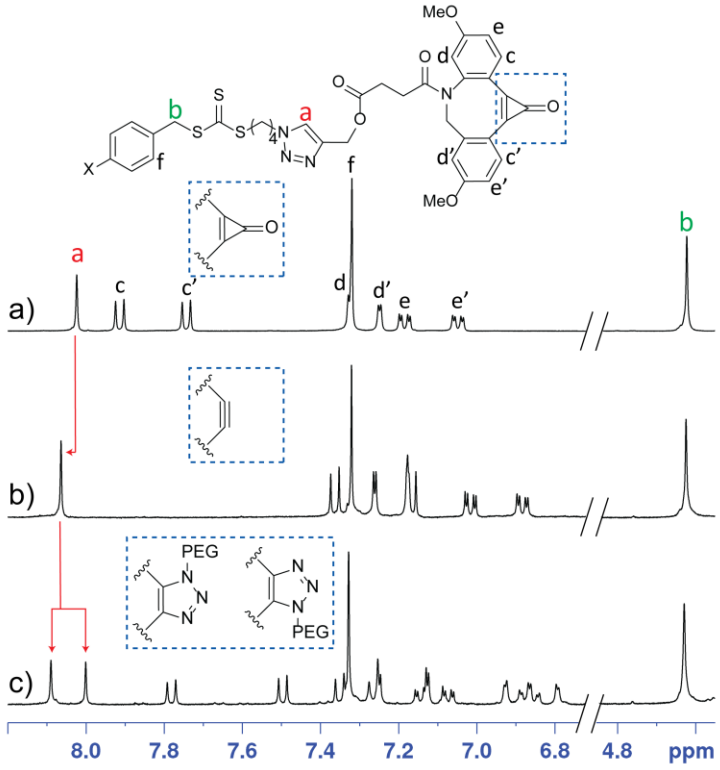

Figure S19. Deprotection and click of 2-arm star RAFT agent (R2) by ^{1}H NMR (*d6*-DMSO). a) Before and b) after deprotection (3 h UV) and c) after addition of 1.0 eq of 400 PEG-N3 with respect to DIBAC.

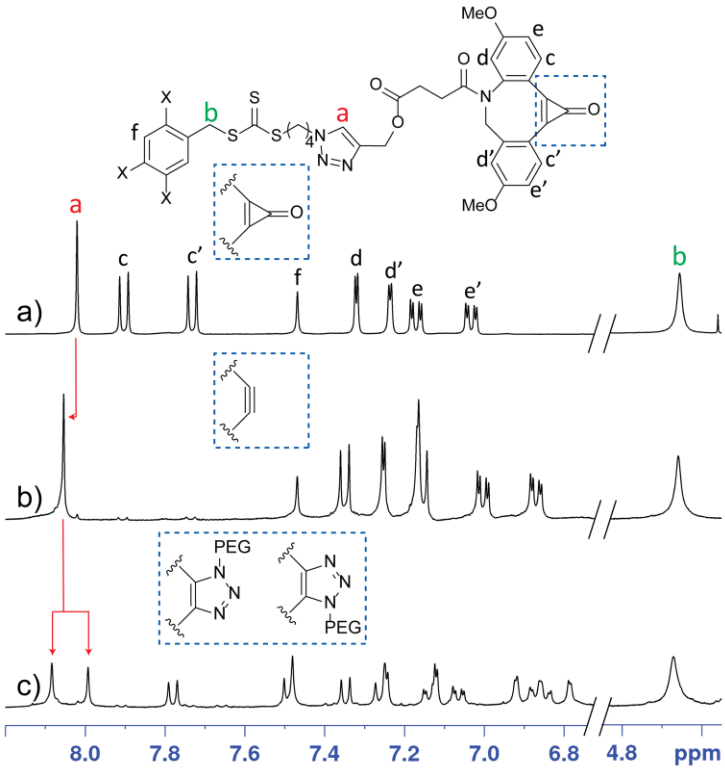

Figure S20. Deprotection and click of 4-arm star RAFT agent (R4) by ^{1}H NMR (*d6*-DMSO). a) Before and b) after deprotection (3 h UV) and c) after addition of 1.0 eq of 400 PEG-N3 with respect to DIBAC.

Peer reviewed version of the manuscript published in final form in the Journal of the American Chemical Society, 2019, DOI: 10.1021/jacs.9b09899

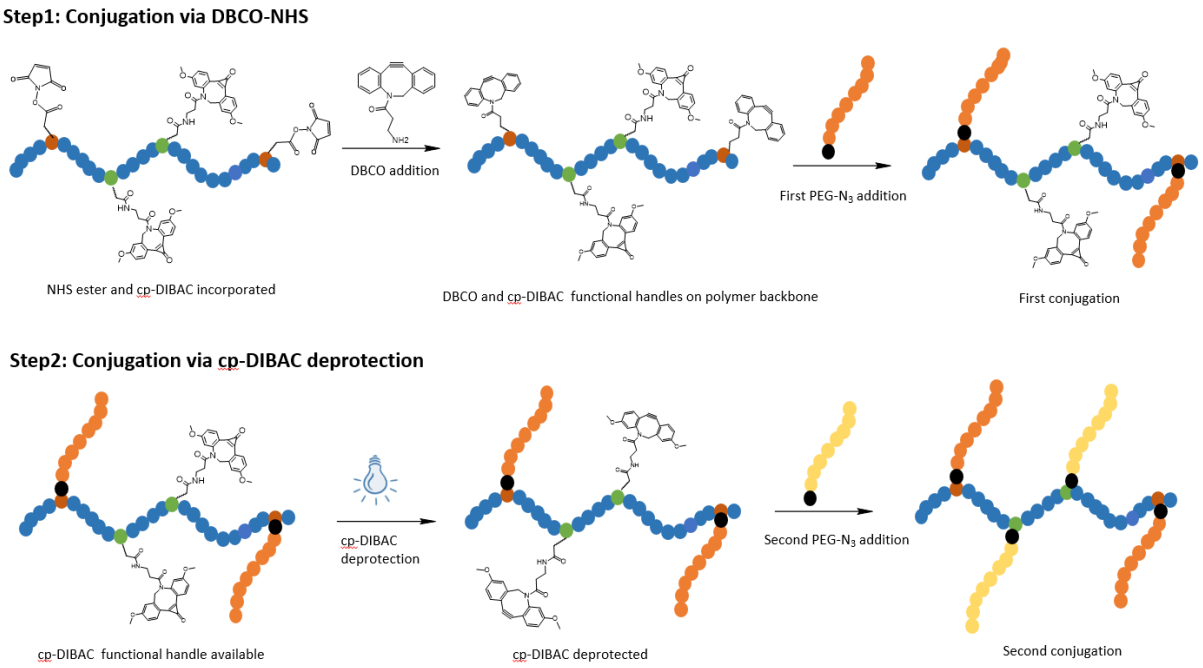

Figure S21. Schematic showing dual functionalization capabilities using DBCO and cp-DIBAC via SPAAC

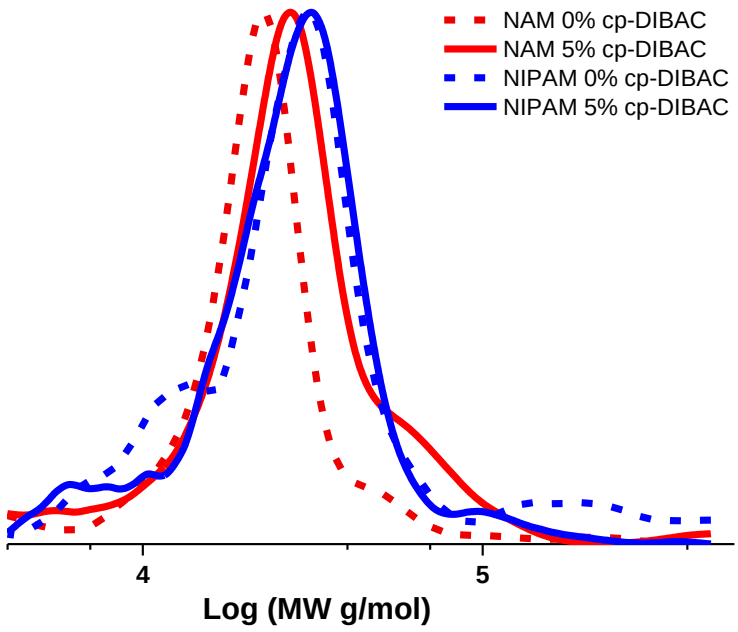

Figure S22. NAM and NIPAM (DP 200) copolymerized with 5% cp-DIBAC monomer shows its compatibility with various monomers.

Peer reviewed version of the manuscript published in final form in the Journal of the American Chemical Society, 2019, DOI: 10.1021/jacs.9b09899

Table S3. GPC characterisation of NAM and NIPAAM linear polymers prepared with 0% and 5% cp-DIBAC (M1).

Monomer	% cp-DIBAC	DP	$M_{n,\,Theo}$	$M_{n,\,GPC}$	$M_{w,GPC}$	$Đ$
NAM	0	200	28.6	19.8	22.3	1.12
NAM	5	200	31.1	24.0	29.0	1.20
NIPAM	0	200	23.0	26.9	30.0	1.11
NIPAM	5	200	26.0	25.1	28.4	1.12

Table S4. Dual conjugation study molecular weight data for DMA DP 200 2.5% DBCO 2.5% cp-DIBAC composition

Polymer	$M_{n,\,Theo}$	$M_{n,GPC}$	$M_{w,GPC}$	$Đ$
DMA 0% NHS 0% cp-DIBAC	20.2	23.1	24.9	1.08
DMA 2.5% NHS 2.5% cp-DIBAC	22.7	23.6	26.1	1.10
First PEG addition		36.0	45.5	1.26
Second PEG addition		43.2	53.7	1.24

Table S5. DMA DP 200 5% cp-DIBAC molecular weight data at various time points

DMA 5% cp-DIBAC (DP 200)	$M_{n,GPC}$	$M_{w,GPC}$	$Đ$
t = 8 h	14.6	15.7	1.08
t = 12 h	19.1	21.8	1.14
t = 16 h	22.9	27.2	1.18

Peer reviewed version of the manuscript published in final form in the Journal of the American Chemical Society, 2019, DOI: 10.1021/jacs.9b09899

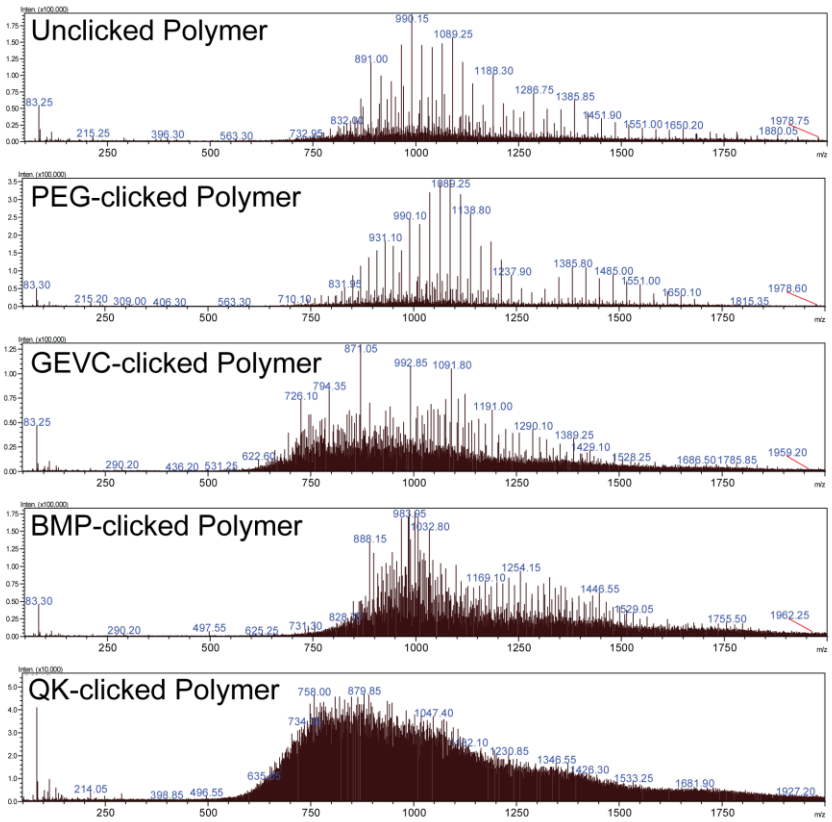

Figure S23. ESI-MS spectra for the 2-arm DMA_{20} polymer peaks shown in Figure 7a before click (○) and after click (●) to PEG-N_3 (400 Da), GEVC, BMP and QK peptides confirming the identity of these peaks.

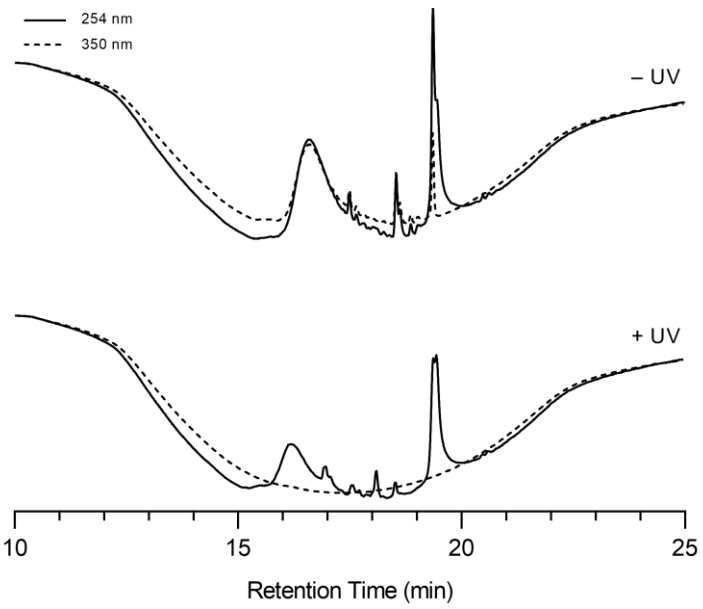

Figure S24. Photodiode array (PDA) detector chromatogram data for the PEG-N_3 (400 Da) traces in Figure 7a at 254 and 350 nm. The loss of signal at 350 nm in the polymer peak can be seen after UV irradiation, consistent with full deprotection of the polymer.

Peer reviewed version of the manuscript published in final form in the Journal of the American Chemical Society, 2019, DOI: 10.1021/jacs.9b09899

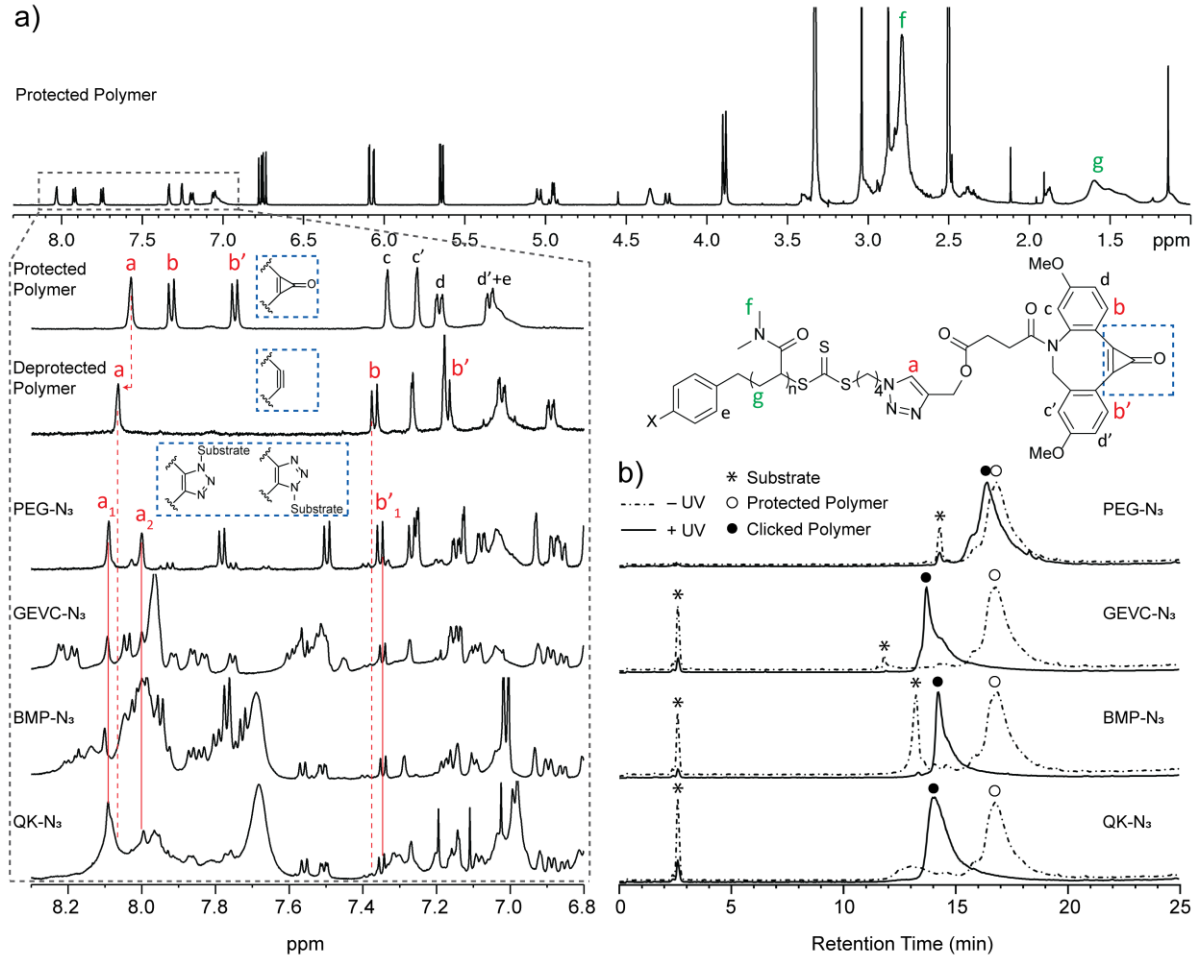

Figure S25. a) ^{1}H-NMR (*d6*-DMSO) for the 2-arm DP20 pDMA shown in Figure 7a (reproduced here as figure b) before and after deprotection, and after click to PEG-N_3 (400 Da), GEVC, BMP and QK peptides.

Peer reviewed version of the manuscript published in final form in the Journal of the American Chemical Society, 2019, DOI: 10.1021/jacs.9b09899

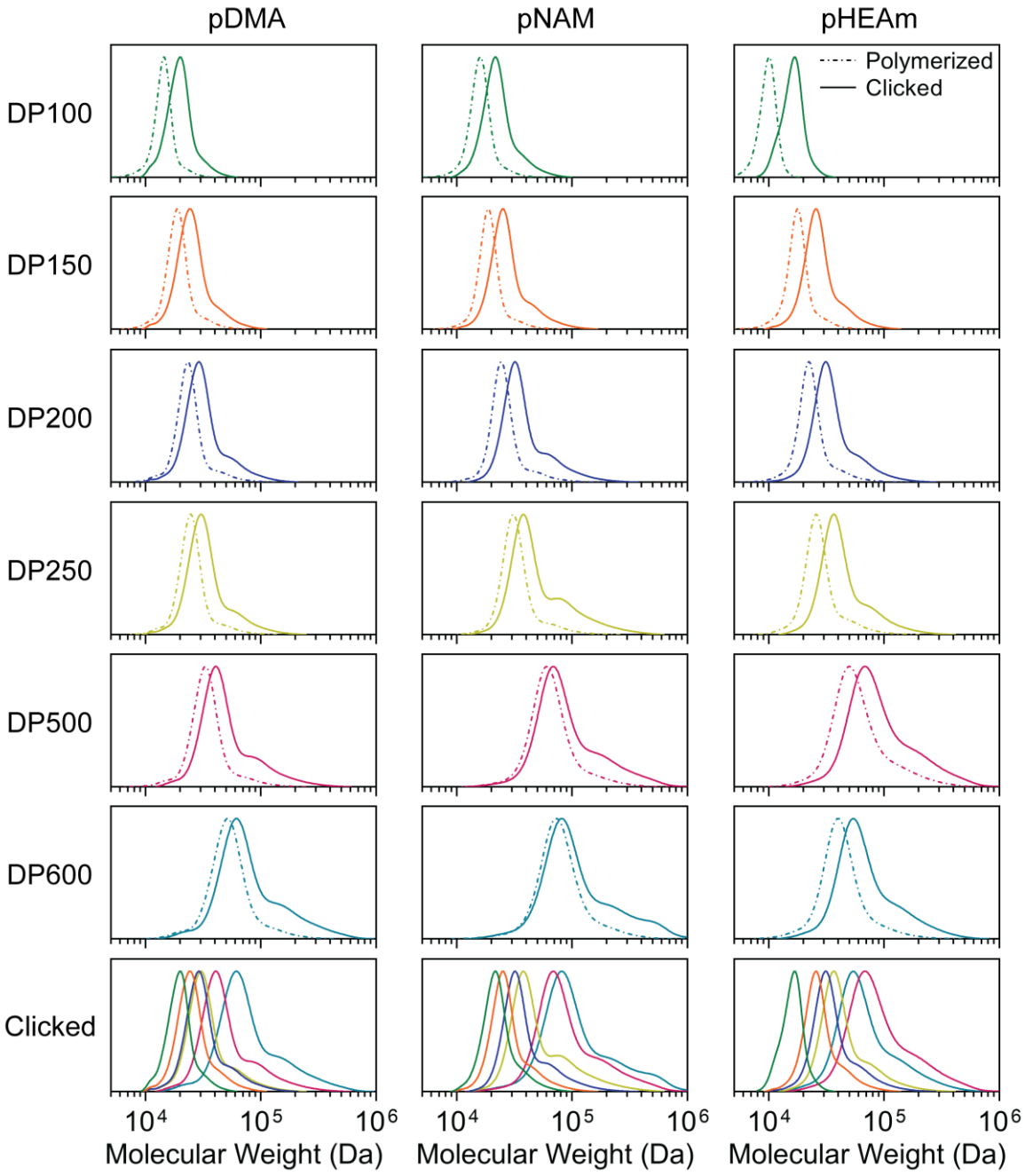

Figure S26. Library of 3-arm polymers. GPC traces of 3-arm star polymer libraries of dimethyl acrylamide (DMA), *N*-acryloyl morpholine (NAM) and 2-hydroxyethyl acrylamide (HEAm) shown in Figure 7b before and after click with PEG-N_3 (2 kDa).

Peer reviewed version of the manuscript published in final form in the Journal of the American Chemical Society, 2019, DOI: 10.1021/jacs.9b09899

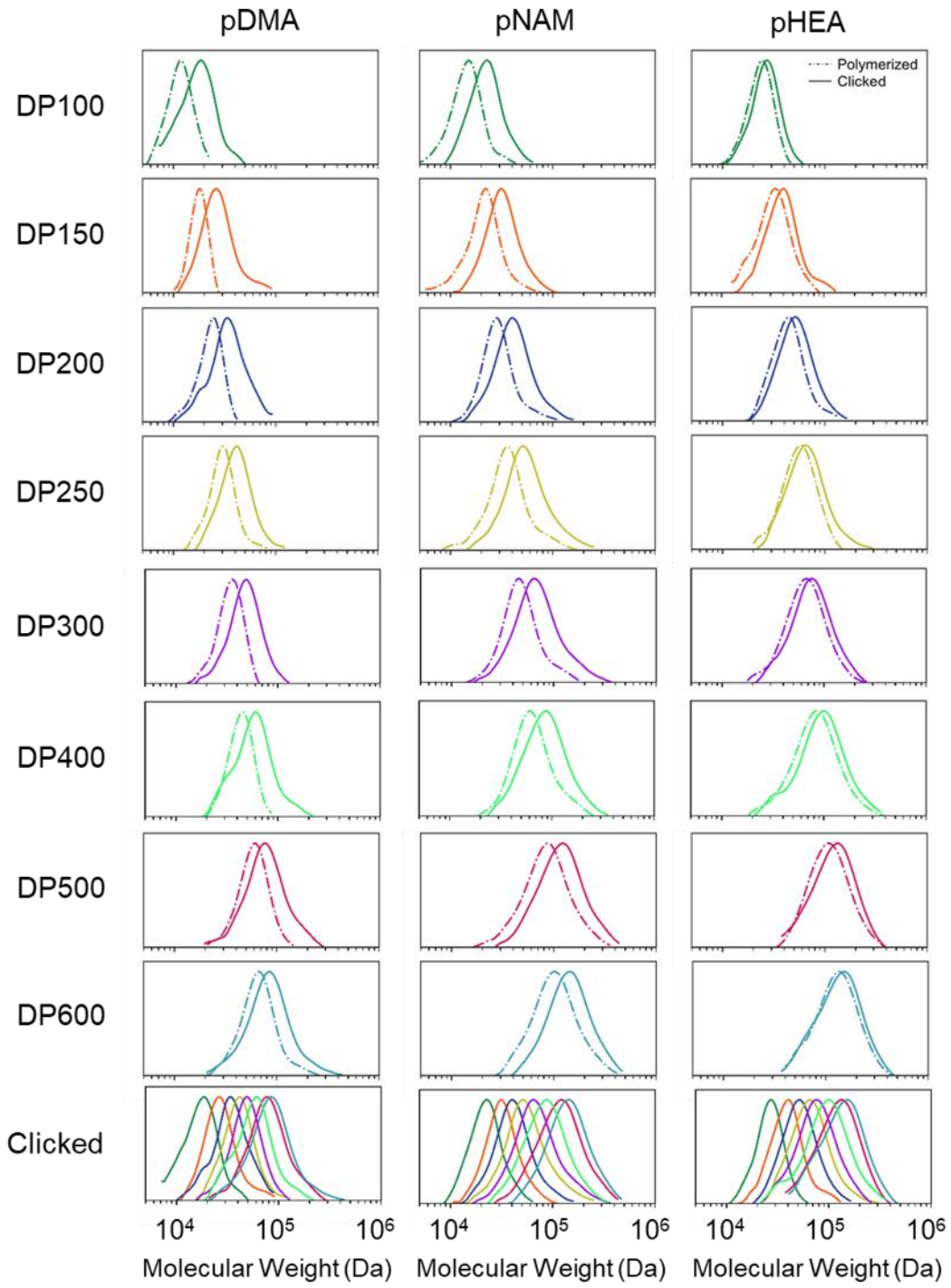

Figure S27. Library of linear polymers. GPC traces of linear polymer libraries of dimethyl acrylamide (DMA), *N*-acryloyl morpholine (NAM) and 2-hydroxyethyl acrylamide (HEAm) shown in Figure 7b before and after click with PEG-N_3 (2 kDa).

Peer reviewed version of the manuscript published in final form in the Journal of the American Chemical Society, 2019, DOI: 10.1021/jacs.9b09899

Table S6. GPC molecular weight (in kDa) and dispersity information for linear and 3-arm library shown in Figure 7

Target DP (total)	DMA				NAM				HEAm			
	Before click		+ PEG-N_3		Before click		+ PEG-N_3		Before click		+ PEG-N_3	
	M_n	Đ	M_n	Đ	M_n	Đ	M_n	Đ	M_n	Đ	M_n	Đ
Linear (5% cpDIBAC)												
100	11.3	1.08	16.0	1.15	13.5	1.13	20.1	1.14	21.6	1.08	25.0	1.10
150	17.2	1.04	24.5	1.12	18.6	1.18	28.3	1.15	27.9	1.15	34.2	1.16
200	20.7	1.11	28.8	1.19	26.5	1.14	35.0	1.20	39.1	1.13	45.2	1.16
250	27.4	1.11	36.4	1.13	29.1	1.27	44.5	1.27	48.1	1.16	56.1	1.22
300	30.9	1.10	40.9	1.16	41.1	1.19	54.5	1.33	53.2	1.26	61.5	1.25
400	40.1	1.08	48.2	1.21	54.4	1.21	68.6	1.28	64.5	1.32	70.4	1.37
500	51.1	1.15	63.5	1.25	62.8	1.35	90.9	1.33	92.7	1.23	99.7	1.27
600	56.1	1.20	67.2	1.30	81.6	1.31	114.3	1.27	103.9	1.26	109.0	1.29
3-arm star												
100	13.8	1.05	18.4	1.07	15.2	1.06	20.6	1.10	9.6	1.03	15.3	1.05
150	17.8	1.07	22.9	1.11	18.0	1.06	24.7	1.14	16.8	1.07	24.6	1.12
200	21.9	1.10	27.7	1.17	23.5	1.10	32.5	1.20	21.2	1.10	30.4	1.18
250	23.0	1.14	28.8	1.18	29.6	1.12	39.9	1.35	24.5	1.13	36.5	1.22
500	30.0	1.15	39.9	1.30	54.4	1.23	67.0	1.46	46.2	1.33	67.0	1.48
600	44.1	1.22	57.7	1.47	63.1	1.29	75.8	1.63	35.1	1.23	52.4	1.39

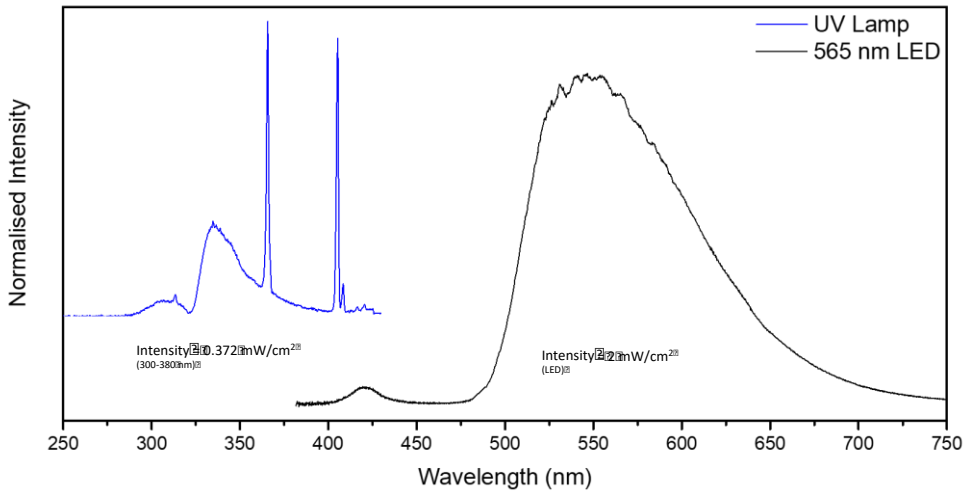

Figure S28. Emission spectra of the Cosmedico ARIMED B6 UV lamp (blue) and the Thorlabs M565L3 LED (black) used for the polymerisation and deprotection of the star polymer systems. The UV power was measured using a 355/40 Thorlabs filter over the power head (blue spectrum) to remove some of the background light. This bandpass allows transmission of 300-380 nm light. Spectra of the lamps used for the linear systems are assumed to be similar but were not measured. Power values for all spectra are included in the manuscript.

Peer reviewed version of the manuscript published in final form in the Journal of the American Chemical Society, 2019, DOI: 10.1021/jacs.9b09899

3. References

(1) Kramer, J. J. P.; Nieger, M.; Bräse, S. Synthesis of Planar Chiral N-Heterocyclic-Substituted Pyridinophanes. *Eur. J. Org. Chem.* **2013**, *2013* (3), 541–549. DOI: https://doi.org/10.1002/ejoc.201201286

Insert Table of Contents artwork here